COMMISSARIAT A L'ENERGIE ATOMIQUE

Centre d'Etudes Nucléaires de Saclay

91191 Gif-sur-Yvette Cedex

DPhPE 87-20

November 1987

TEST OF THE STANDARD MODEL WITH WEAK BOSONS IN UA1

C. STUBENRAUCH

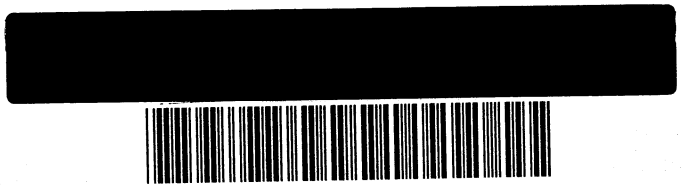

CM-P00062934

Talk given at the International Symposium on "High Energy Experiments and Methods" HEXAM-87, Bechyne Castle, 14-19 September 1987.

DEPARTEMENT DE PHYSIQUE DES PARTICULES ELEMENTAIRES

TEST OF THE STANDARD MODEL WITH WEAK BOSONS IN UA1

UA1 COLLABORATION
CERN, Geneva, Switzerland.

Presented by C. STUBENRAUCH
DPhPE, CEN-Saclay
91191 Gif-sur-Yvette Cedex, France.

Abstract :

Since the discovery in 1983 of the intermediate vector bosons W and Z, the number of events has considerably increased so that one can now study their properties more precisely. All physics aspects are covered, with particular emphasis on the tests of QCD through the W,Z production properties. The experimental distributions investigated confirm everywhere Standard Model (electroweak and QCD) expectations at $Q^2 = M_W^2$.

1 - INTRODUCTION

Since 1982 the UA1 experiment has accumulated about 400 W events and 50 Z° events decaying into lepton pairs, which corresponds to an integrated luminosity of about 700 nb^{-1}. With these samples we now have a good tool to test both the electroweak and the QCD aspects of the Standard Model, and this at very high $Q^2 \simeq M_W^2$.

The UA1 apparatus has been extensively described in [1]. For illustration we just show the side view of the experiment in fig. 1.

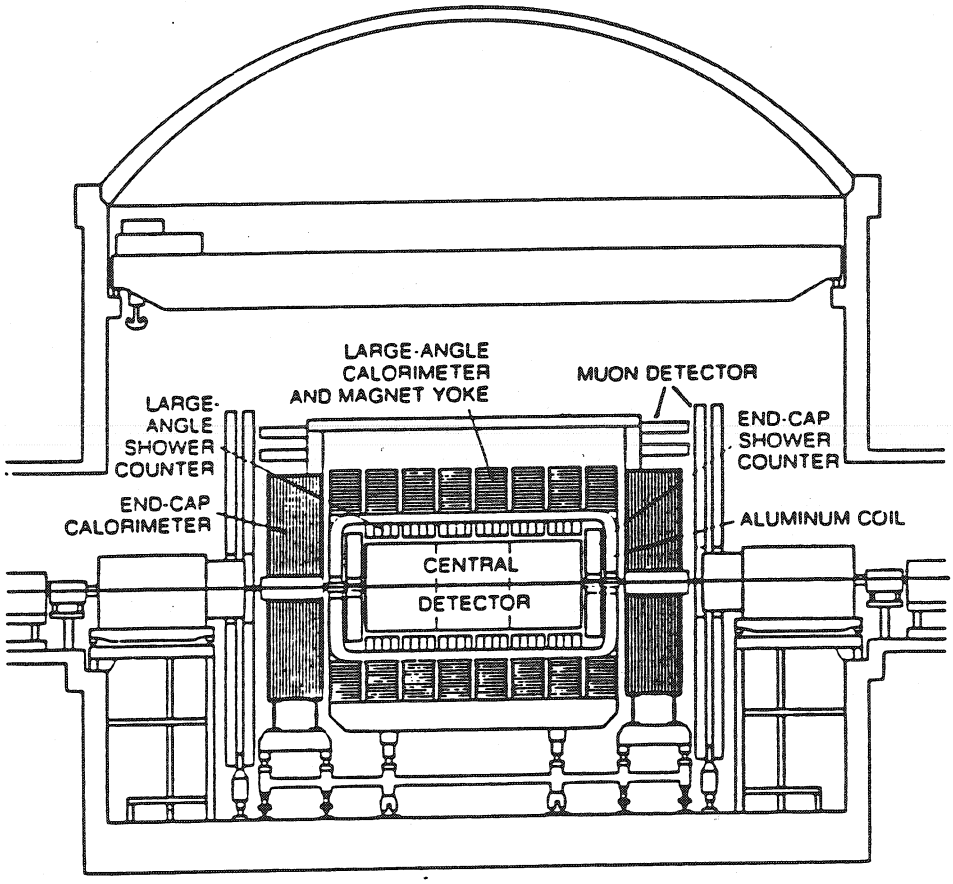

Fig. 1 : Side view of the UA1 detector.

Table 1

UA1 event samples, efficiencies, backgrounds, and integrated luminosities

$\sqrt{s}$ (GeV)	Channel	Events	Background events	Efficiency	Integrated luminosity (nb^{-1})
546	$W \to e\nu$	59	6.8 ± 2.0	0.69 ± 0.03	136 ± 20
	$W \to \mu\nu$	10	0.70 ± 0.10	0.16 ± 0.02	108 ± 16
	$Z^0 \to e^+e^-$	4	< 0.1	0.69 ± 0.03	136 ± 20
	$Z^0 \to \mu^+\mu^-$	4	0.07 ± 0.03	0.37 ± 0.05	108 ± 16
630	$W \to e\nu$	240	19.3 ± 1.7	0.61 ± 0.02	568 ± 85
	$W \to \mu\nu$	57	3.3 ± 0.5	0.15 ± 0.01	551 ± 83
	$Z^0 \to e^+e^-$	29	0.2 ± 0.02	0.69 ± 0.02	568 ± 85
	$Z^0 \to \mu^+\mu^-$	15	< 0.5	0.40 ± 0.02	555 ± 83
546/630	$W \to \tau\nu$	32	2.7 ± 0.6	0.068 ± 0.004 $\pm 0.007^{*)}$	686 ± 103

*) This additional systematic error is due to the uncertainty on energy scale and tau selection.

2 - DATA SAMPLES

A summary of the W and Z data samples collected in UA1 at the two energies $\sqrt{s}$ = 546 GeV and $\sqrt{s}$ = 630 GeV is given in table 1, together with their associated selection efficencies, backgrounds and integrated luminosities. Details of the W and Z selection procedures can be found in [2, 3, 4, 5]. Here we just mention the principle of the selections.

W decays in the $e\nu$ and $\mu\nu$ channels are selected by requiring the presence of an isolated charged lepton (electron or muon) with transverse energy in excess of 15 GeV produced in association with a missing transverse energy (neutrino) in excess of 15 GeV. The signature for an electron is provided by an isolated track in the central detector, the longitudinal shower profile in the electromagnetic and hadronic calorimeters and the matching between the track of the electron candidate

and its shower in the calorimeter. The muon is detected as an isolated track in the central detector and the muon chambers, the amount of matter between these two detectors corresponding to more than $\sim$ 8 interaction lengths. In addition, to eliminate background from bijet events, events with a jet back-to-back (within 30°) to the muon candidate are not taken into account.

The $W \to \tau\nu \to$ hadrons $\bar{\nu}\nu$ events are more difficult to detect, therefore an additional validation of the missing transverse energy is required and a cut $E_T^{miss} \geq 4\sigma$ (with $\sigma = 0.7\sqrt{\Sigma|E_T^i|}$) is applied. The tau candidate is selected as a low multiplicity, collimated jet with $E_T^{jet} > 12$ GeV. Then a τ-likelihood is formed on the basis of several parameters including collimation, multiplicity and track-shower matching of the jet.

Z events decaying into two electrons are selected by requiring the presence of two isolated electrons with transverse energy in excess of 8 GeV, and a two-electron mass larger than 70 GeV/c^2.

Z events decaying into two muons are selected by requiring an isolated muon with an additional isolated track with transverse momentum in excess of 15 GeV/c produced in association with transverse momentum larger than 15 GeV/c. To exclude low mass Drell-Yan pairs the invariant mass of the muon pair is required to be larger than 50 GeV/c^2.

2.1 e-μ-τ universality

The results on production cross-sections are given in table 2 for all decay channels, where they are compared to the measured values of UA2 [6] and to theoretical predictions [7]. All experimental values are in good agreement within the errors. (These cross-sections are discussed in the context of QCD in more detail in section 4.1.)

The good agreement of the W production results in the 3 different decay channels of electron, muon and tau is a very nice verification of

lepton universality for weak charged currents at $Q^2 = M_W^2$.

More precisely, we obtain the following ratios (where the systematic errors of 15 % on the luminosity cancel out) at $\sqrt{s}$ = 630 GeV :

$$R^{cc}_{\mu/e} \equiv \frac{\sigma.B(W \to \mu\nu)}{\sigma.B(W \to e\nu)} = 1.00 \pm 0.15 \pm 0.08$$

$$R^{cc}_{\tau/e} \equiv \frac{\sigma.B(W \to \tau\nu)}{\sigma.B(W \to e\nu)} = 1.02 \pm 0.20 \pm 0.10$$

This is the first direct test of lepton universality in weak charged currents at $Q^2 = M_W^2$.

In the same way, the agreement between $\sigma(Z^\circ \to e^+e^-)$ and $\sigma(Z^\circ \to \mu^+\mu^-)$ is a test for lepton universality in weak neutral currents at $Q^2 = M_Z^2$. With the data at $\sqrt{s}$ = 630 GeV, we have :

$$R^{NC}_{\mu/e} \equiv \frac{\sigma.B(Z \to \mu\mu)}{\sigma.B(Z \to ee)} = 0.91 \pm 0.29 \pm 0.06$$

Table 2

Production cross-sections of W and Z

	$\sqrt{s}$ (GeV)	546	630
UA1	σ_W^e (nb)	$0.53 \pm 0.08 \pm 0.09$	$0.61 \pm 0.04 \pm 0.09$
	σ_W^μ (nb)	$0.54 \pm 0.17 \pm 0.12$	$0.61 \pm 0.09 \pm 0.11$
	σ_W^τ (nb)		$0.63 \pm 0.13 \pm 0.12$
UA2	σ_W^e (nb)	$0.61 \pm 0.10 \pm 0.07$	$0.57 \pm 0.04 \pm 0.07$
theory	σ_W^ℓ (nb)	$0.36 \,^{+\,0.11}_{-\,0.05}$	$0.47 \,^{+\,0.14}_{-\,0.08}$
UA1	σ_Z^e (pb)	$42 \,^{+\,33}_{-\,20} \pm 6$	$74 \pm 14 \pm 11$
	σ_Z^μ (pb)	$98 \,^{+\,78}_{-\,46} \pm 20$	$66 \pm 17 \pm 10$
UA2	σ_Z^e (pb)	$116 \pm 39 \pm 11$	$73 \pm 14 \pm 7$
theory	σ_Z^ℓ (pb)	$42 \,^{+\,13}_{-\,6}$	$51 \,^{+\,16}_{-\,8}$

2.2 Light neutrino counting

The measured cross sections $(\sigma.B)_{W,Z}$ can be exploited to derive an upper limit on the number of neutrino generations (where the neutrino mass is much smaller than half the Z° mass), or more generally, on the number of fermion families. The observed number of $Z \to \ell\bar{\ell}$ decays is sensitive to the total number of open decay channels $Z \to \nu_i \bar{\nu}_i$. By considering the ratio R :

$$R_{exp} = \frac{N(W \to \ell\nu)}{N(Z \to \ell\ell)}\Bigg|_{exp} = \frac{\sigma_W.B(W \to \ell\nu)}{\sigma_Z.B(Z \to \ell^+\ell^-)}$$

in which the systematic errors due to the $\sim$ 15 % uncertainty on the luminosity cancel, one can then determine ΔN_ν, the number of neutrinos in excess of the three known.

The measured value of R_{exp} can be compared to the value of R predicted by the Standard Model :

$$R_{theo} = \underbrace{\frac{\sigma_W}{\sigma_Z}}_{R_\sigma} \cdot \underbrace{\frac{\Gamma(W \to \ell\nu)}{\Gamma(Z \to \ell^+\ell^-)} \cdot \frac{\Gamma_Z^{tot}}{\Gamma_W^{tot}}}_{R_\Gamma}$$

under several hypotheses on the number of neutrino generations and as a function of the top quark mass [8].

The ratio R_σ of the W to Z production cross sections can be calculated in QCD but is affected by theoretical uncertainties on the one hand due to the choice of structure funtions and of Λ, and on the other hand due to the W and Z masses, i.e. $\sin^2\theta_W$.

Several theoretical approaches have been made to calculate R_σ using different structure function parametrizations. In 1984, Altarelli et al. [7] have obtained : $R_\sigma = 3.25 \pm 0.20$ (at $\sqrt{s}$ = 630 GeV) using DO1 and GHR structure functions which are largely based on the old data of CDHS. More

recently, Martin et al. [9] have adjusted the ratio $F_2^{\mu n}(x)/F_2^{\mu p}(x)$ on the data of EMC. This ratio is essentially a function of the ratio d(x)/u(x) of the u and d quark momentum distributions. Using the world average value for $\sin^2\theta_w$: 0.232 ± 0.004 ± 0.003 and taking into account some theoretical uncertainties, they find : R_σ = 3.36 ± 0.09. The systematic error on the EMC data in the determination of F_2^n/F_2^p is neglected,however it is the dominant one. Most recently, Martinelli et al. [10] find R_σ = 3.28 ± 0.15 by using all available structure function measurements in ν, $\bar{\nu}$ deep inelastic scattering. Another fit [8] based on the most recent BCDMS data [20] was made with the result : R_σ= 3.23 ± 0.15 taking into account also the systematic errors. Fig. 2. shows the ratio $F_2^n(x)/F_2^p(x)$ measured by BCDMS as a function of x in comparison to the same ratio calculated with the parametrizations GHR, DO1, EHQL1 and Martin et al.. The x domain corresponding to the W and Z produced at the collider is concentrated around $\langle x\rangle = M_{W,Z}/\sqrt{s} \cong 0.15$ (see fig. 16).

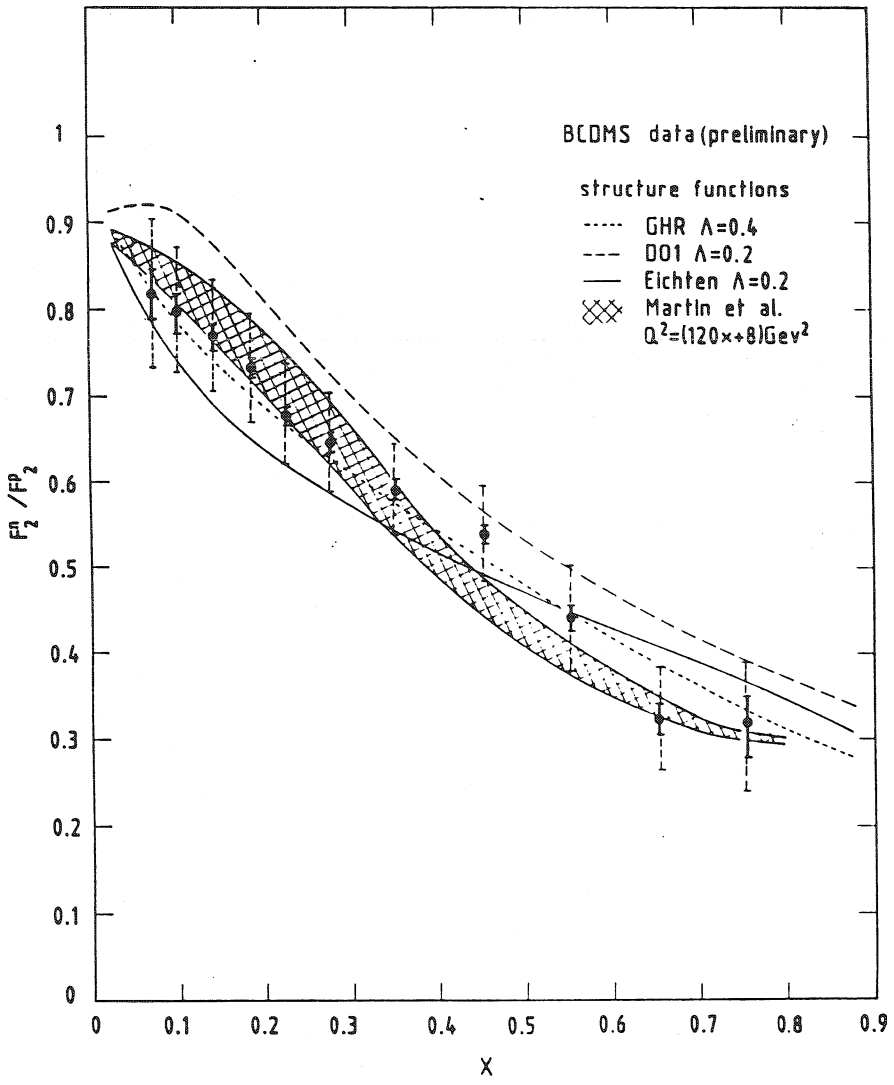

Fig. 2 :

Ratio $F_2^n(x)$ / $F_2^p(x)$ measured by BCDMS as a function of x in comparison to the same ratio calculated with the parametrisation GHR, DO1, EHQL1 and Martin et al.

The uncertainties on R_σ can be given by the two extreme values found for R_σ of 3.36 and 3.10.

The ratio of the partial decay widths R_Γ is predicted by the Standard Model and depends essentially on the boson masses M_W and M_Z. In addition, the total decay widths are sensitive to the top quark mass m_{top} through the decay channels $W \to t\bar{b}$ and $Z \to t\bar{t}$, and Γ_Z^{tot} increases by $\Delta\Gamma(Z \to \nu_i \bar{\nu}_i) = \frac{G_F}{12\pi\sqrt{2}} M_Z^3$ ($\simeq$ 170 MeV) for each additional neutrino family. Assuming that there is no additional heavy lepton with a mass lower than the W mass and by choosing $\sin^2\theta_W = 0.230$, $\Lambda = 0.26$ GeV, $N_\nu = 3$ and $m_{top} = 40$ GeV/c^2 we get $R_\Gamma = 2.7$. A variation of $\pm$ 0.010 for $\sin^2\theta_W$ and of $\pm$ 0.1 GeV for Λ provides a change of R_Γ only of $\pm$ 0.01, negligeable compared to the error on R_σ.

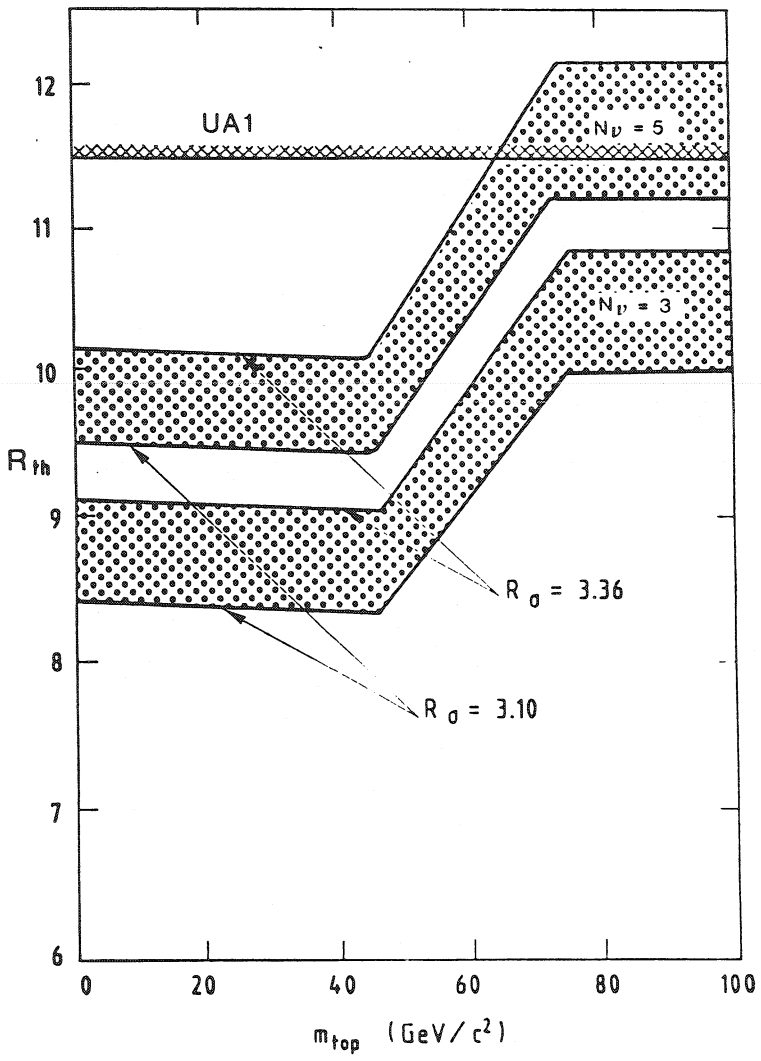

Fig. 3 : R as a function of the top quark mass with 2 hypotheses on the number of neutrino families (N_ν = 3 or 5). The hatched area corresponds to the uncertainty of R_σ. Also indicated the experimental upper limit of R measured by UA1.

Fig. 3 shows the theoretical value $R = R_\sigma \cdot R_\Gamma$ as a function of the top quark mass with 2 hypotheses on the number of neutrino families (N_ν = 3 or 5). The hatched areas correspond to the uncertainty of R_σ discussed above.

The experimental value of R measured by UA1 alone is [11] :

$$R_{exp} = 9.1 \ ^{+\ 1.7}_{-\ 1.2}$$

which leads to an upper limit of :

$$R_{exp} < 11.5 \qquad \text{at} \qquad 90\ \%\ \text{C.L.}$$

This value is indicated in fig. 3, where we can see that the number of neutrino families is $\lesssim 5$ for a top mass higher than 70 GeV/c.

By using the upper limit on the total Z decay width :

$$\Gamma^{sup}_{Z,tot}\ (m_{top}) = \frac{R^{sup}_{exp}}{R_\sigma} \cdot \frac{\Gamma^{Z}_{\ell\ell}}{\Gamma^{W}_{\ell\nu}} \cdot \Gamma^{W}_{tot}\ (m_{top})$$

we obtain directly the number of additional neutrino families ΔN_ν :

$$\Delta N_\nu = N_\nu - 3 < (\Gamma^{sup}_{Z,tot}\ (m_{top}) - \Gamma^{3\ gen}_{Z,tot}\ (m_{top}) \ / \ \Gamma^{Z}_{\nu\nu}$$

where $\Gamma^{3\ gen}_{Z,tot}\ (m_{top})$ is the total Z° width expected theoretically for 3 neutrino generations.

Fig. 4 shows the upper limit N_ν on the number of neutrino generations as function of the top quark mass for the "pessimistic" value R_σ = 3.10 for the R_{exp} value measured by UA1 (90 % C.L.). By taking into account also the information on R_{exp} provided by UA2 [14], the limit on the number of neutrino generations is 6 for a small top mass ($\lesssim$ 40 GeV/c²) and decreases to 3 for a large top mass ($\gtrsim M_W$) (95 % C.L.).

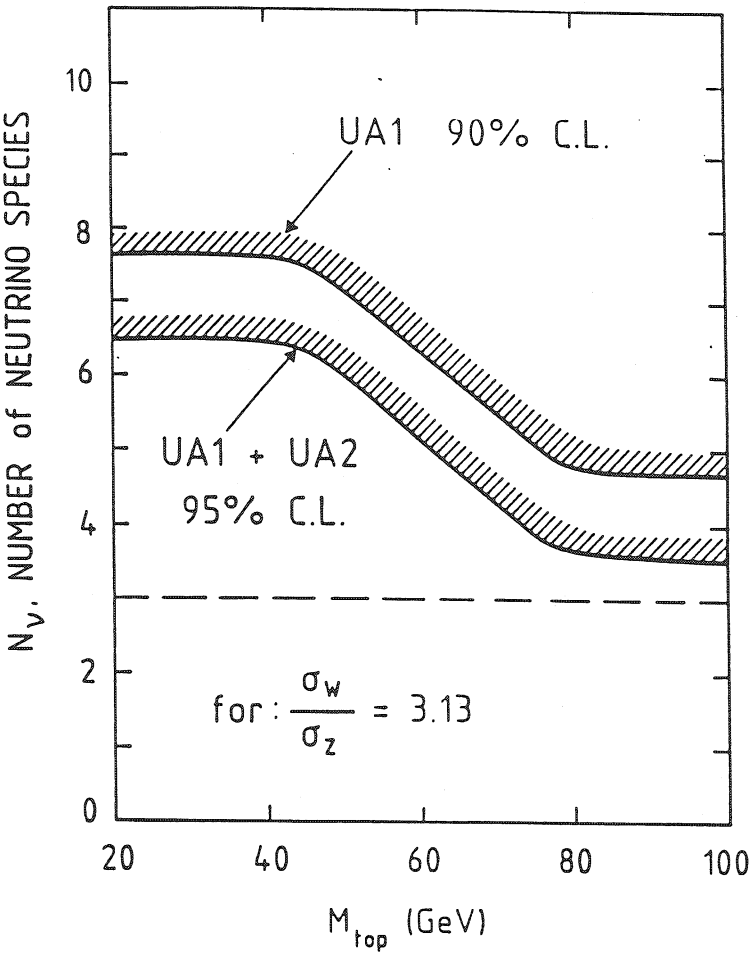

Fig. 4 : Upper limit N_ν on the number of neutrino generations as a function of the top quark mass obtained from UA1 data and from combined UA1 and UA2 data.

3 - TESTS OF THE ELECTROWEAK SECTOR

3.1 Masses and Standard Model parameters

The W and Z masses are obtained independently for the different decay channels. The Z° mass is determined by performing a maximum likelihood fit of a Breit Wigner smeared by experimental resolution on the dilepton mass distribution. Fig. 5 shows this distribution for the well measured Z°events a) in the electron channel and b) in the muon channel. The final UA1 results are [12,13] :

M_z (e^+e^-) = 93.1 ± 1.0 ± 3.1 GeV/c^2 with Γ_z < 5.2 GeV/c^2 at 90 % C.L.

M_z $(\mu^+\mu^-) = 90.7 \,^{+\,5.2}_{-\,4.8} \pm 3.2$ GeV/c^2

The systematic errors are due to the uncertainty in the absolute energy scale. There is good agreement for the Z mass as determined from the two channels as well as with the measured Z mass from UA2 [14] : 92.1 ± 1.1 ±1.5 GeV/c^2 with Γ_z < 5.8 GeV/c^2 (90 % C.L.).

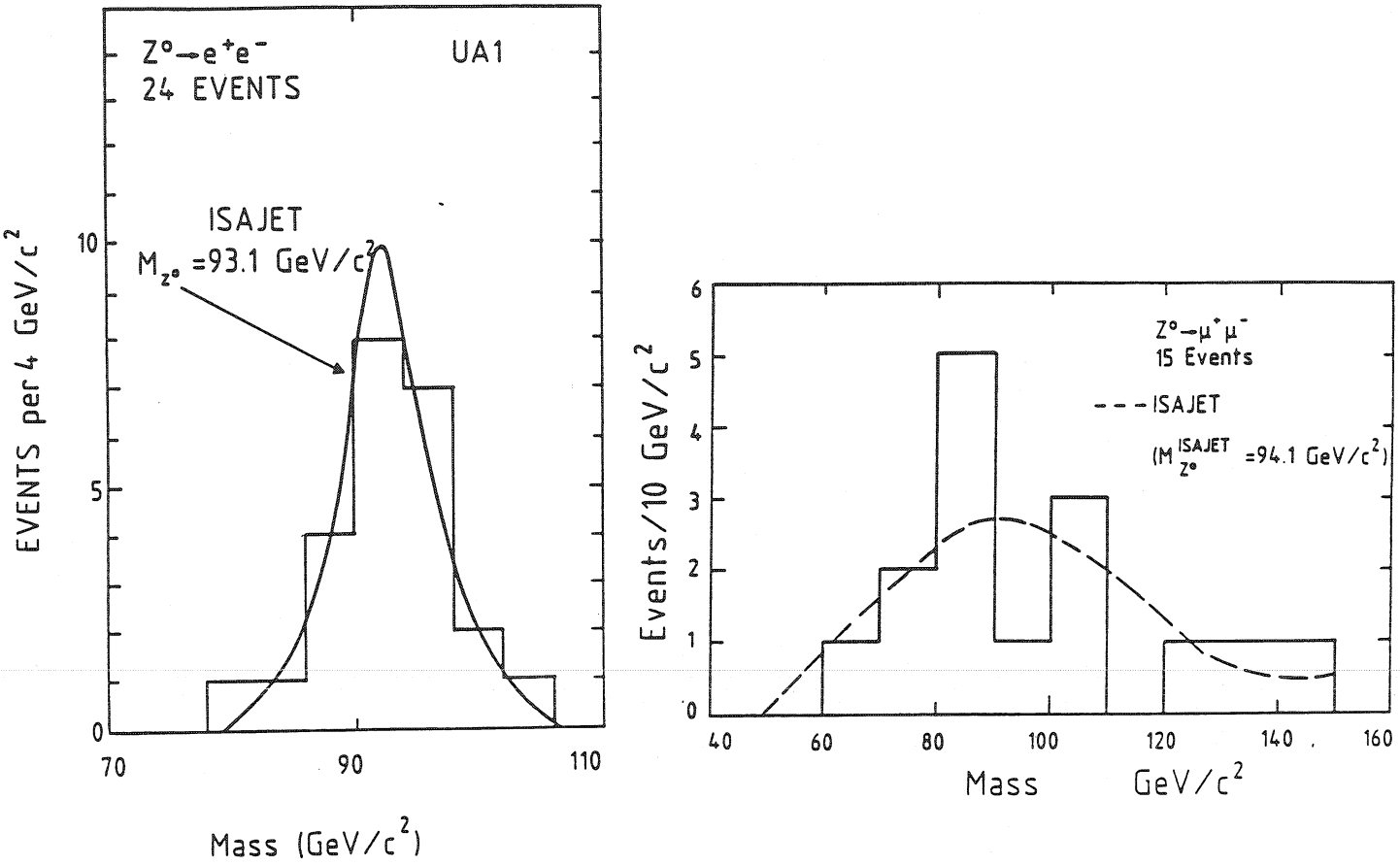

Fig. 5 : Experimental dilepton mass distributions with the results of the Z° mass fit
a) in the electron channel, b) in the muon channel.

In the W case the invariant mass of the $\ell\nu$- system cannot be reconstructed directly from the two body decay fragments since only the transverse momentum of the neutrino is measured. The distribution of the transverse mass :

$$m_T^{e\nu} = \left[2\, E_T^{e} \cdot E_T^{\nu} \cdot (1 - \cos\Delta\varphi^{e\nu})\right]^{1/2}$$

is used to evaluate the W mass. A Monte Carlo simulation which takes into account conventional V-A decay, the expected W longitudinal and transverse momentum and detector characteristics is used with free parameters M_W and Γ_W to fit the data.

Again, for the determination of the mass, only W events with a well measured electron (muon) and neutrino are used (which excludes events with leptons in the vertical region of the detector). To eliminate the background in the electron channel we take into account only W events with the lepton transverse energies in excess of 30 GeV. For the mass fit in the muon sample, we choose the inverse transverse mass distribution rather than the transverse mass itself, because $1/m_T$, being proportional to the curvature of the muon track, most directly reflects the quantity used in the momentum determination and thus simplifies error handling. In the case of $W \to \tau\nu$ events all 32 events are used to fit the W mass.

Figs. 6 a) and c) show the experimental transverse mass distributions in the electron and tau channels and 6 b) the inverse transverse mass distribution in the muon channel with the transverse mass fit from the Monte Carlo.

The final UA1 results are [12,13] :

$M_W\ (e\nu) = 82.7 \pm 1.0 \pm 2.7\ \mathrm{GeV/c^2}$ with $\Gamma_W \leq 5.4\ \mathrm{GeV/c^2}$ (90 % C.L.)

$M_W\ (\mu\nu) = 81.8^{+\,6.0}_{-\,5.3} \pm 2.6\ \mathrm{GeV/c^2}$

$M_W\ (\tau\nu) = 89 \pm 3 \pm 6\ \mathrm{GeV/c^2}$

Again, the systematic errors are dominated by the uncertainty in the absolute energy scale. The mass measurements in the three channels are in good agreement within their errors and they are also compatible with the measured W mass from UA2 [14] : $80.1 \pm 0.8 \pm 1.3\ \mathrm{GeV/c^2}$ with $\Gamma_W \leq 7.0\ \mathrm{GeV/c^2}$ (90 % C.L.).

Fig. 6 : Experimental transverse mass distributions with the results of the W mass fit

a) in the electron channel,

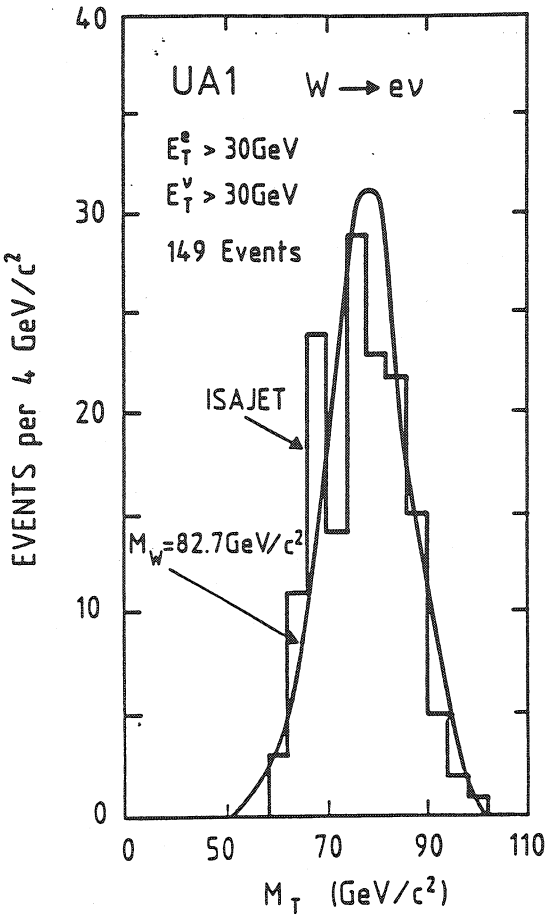

b) inverse transverse mass in the muon channel,

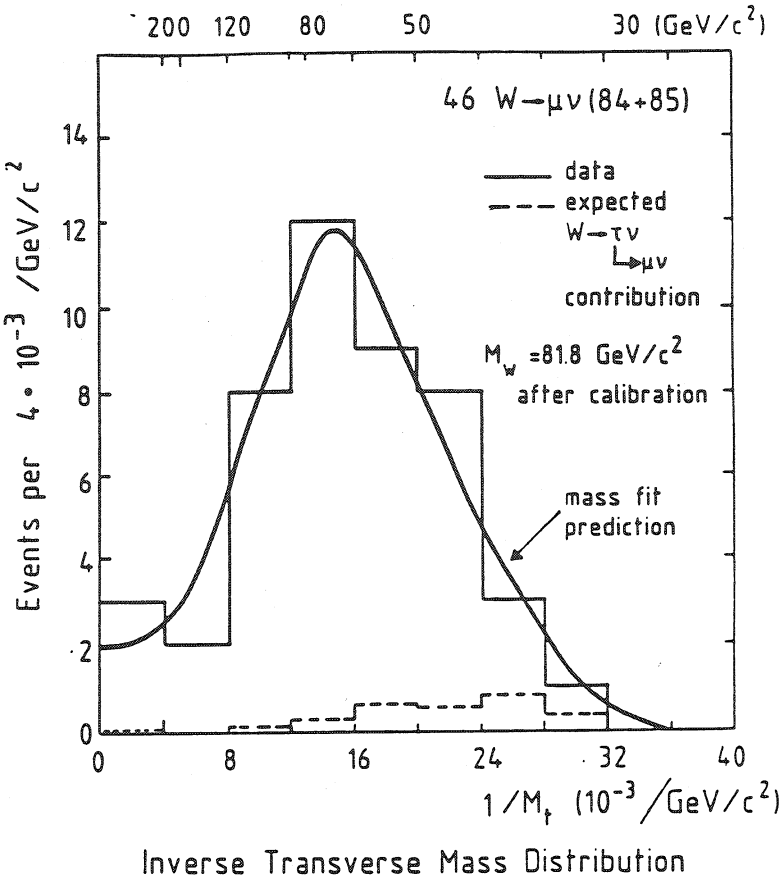

Inverse Transverse Mass Distribution

c) in the tau channel.

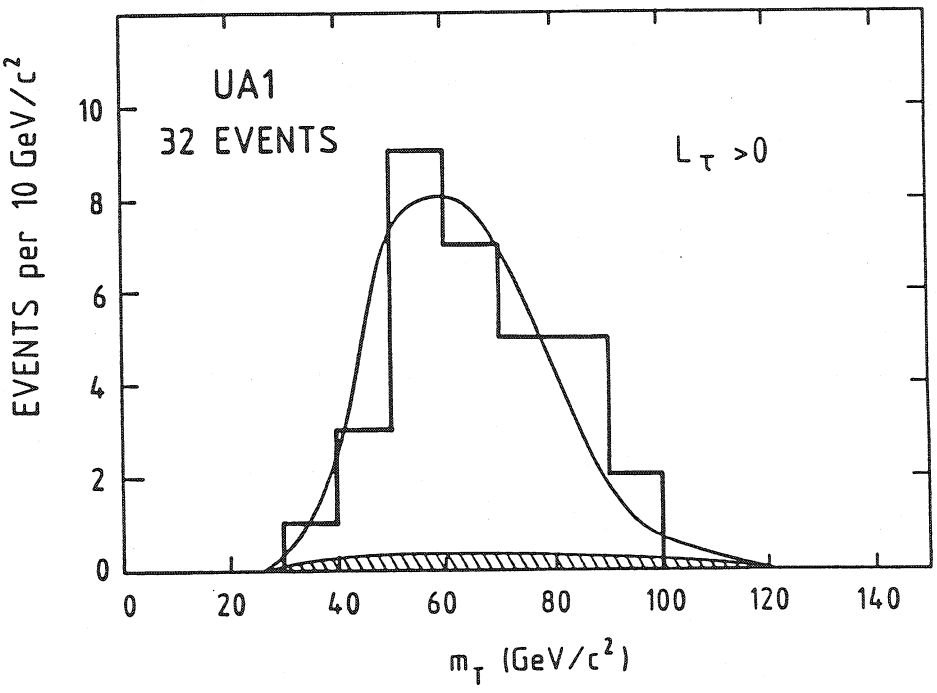

The Standard Model predicts in lowest order a W mass of $\sim$ 78 GeV/c^2 and a Z mass of $\sim$ 89 GeV/c^2. The first order electroweak radiative corrections increase these values by $\Delta r/2$, where Δr is shown in fig. 7 as a function of the top mass and for different values of the Higgs mass [15]. For $m_{top} \lesssim 100$ GeV/c^2 we have $\Delta r/2 \simeq 3.5$ %. The data are in good agreement with these predictions, in particular they are in favour of an increase due to radiative corrections. However, the errors are still too large to test quantitatively these corrections.

Directly related to the boson masses are the Standard Model parameters $\sin^2\theta_W$ and ρ. Two methods are used to determine $\sin^2\theta_W$:

First, one can directly measure $\sin^2\theta_W$ by :

$$(1) \quad \sin^2\theta_W = 1 - M_W^2 / M_Z^2$$

The systematic errors from the energy scale largely cancel out in the mass ratio, but this measurement is limited by the statistical error on M_Z.

The second method is using additional information on α and G_F from low-energy measurements and from calculations of the radiative correction Δr :

$$(2) \quad \sin^2\theta_W = A^2 \left(\frac{1}{1 - \Delta r}\right) \cdot \frac{1}{M_W^2}$$

with $A = \left(\frac{\pi\alpha}{\sqrt{2}\, G_F}\right)^{1/2} = 37.28\ 10 \pm 0.0003$ GeV [16] and $\Delta r = 0.0711 \pm 0.0013$ (for $m_{top} = 35$ GeV/c^2, $m_H = 100$ GeV/c^2, see fig. 7) [15].

The results are summarized in table 3 and are in good agreement with the world average value of $\sin^2\theta_W$ obtained by neutrino scattering experiments [17] : $\sin^2\theta_W = 0.232 \pm 0.004 \pm 0.003$.

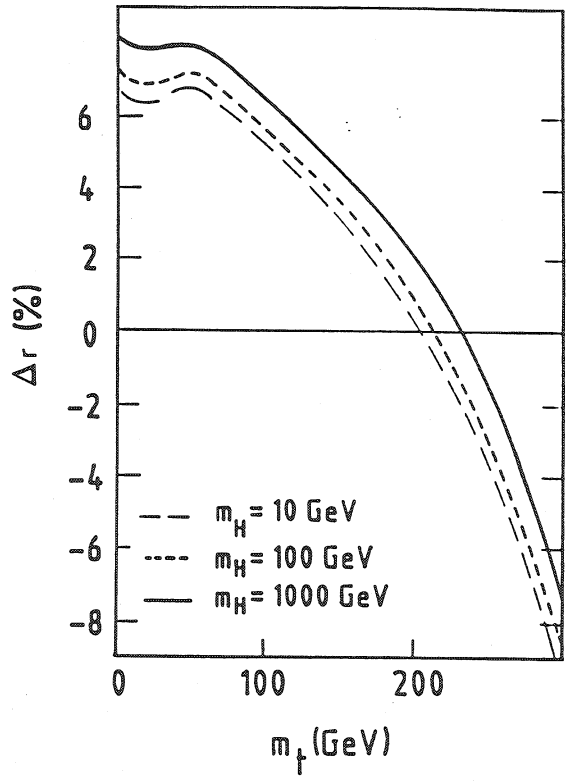

Fig. 7 : Radiative correction Δr as a function of the top quark mass and for different values of the Higgs mass [15].

Table 3

Standard Model parameters

	$\sin^2\theta_w$ (1)	$\sin^2\theta_w$ (2)	ρ
UA1			
e-mode	0.211 ± 0.025	$0.218 \pm 0.005 \pm 0.014$	$1.009 \pm 0.028 \pm 0.020$
μ-mode	$0.187 \pm 0.148 \pm 0.033$	$0.223 \pm {}^{0.033}_{0.029} \pm 0.014$	$1.05 \pm 0.16 \pm 0.05$
UA2			
e-mode	$0.232 \pm 0.025 \pm 0.010$	$0.232 \pm 0.003 \pm 0.008$	$1.001 \pm 0.028 \pm 0.006$
ν-scattering	$0.232 \pm 0.004 \pm 0.003$		

Finally, the parameter ρ is defined as :

$$\rho = M_W^2 \; / \; (M_Z^2 . \sin^2\theta_W)$$

It is predicted to be 1 in the Standard Model, supposing only one Higgs doublet and neglecting small radiative corrections. The UA1 as the UA2 measurements of ρ don't show any significant deviation from the value 1, as one can see in table 3.

3.2 Decay angular distribution of the W.

In the Standard Model, the W is coupled only to lefthanded fermions and righthanded antifermions (neglecting their mass). At our energy of $\sqrt{s}$ = 630 GeV, the average longitudinal momentum fraction of quarks and antiquarks fusing into a W is quite large ($\langle x_{q\bar{q}}^{W} \rangle$ = 0.15) and therefore, most of the W's are produced by the annihilation of a quark coming from the proton and an antiquark coming from the antiproton. Hence, the produced W's are almost totally spin-aligned along the beam direction, and the subsequent $W \rightarrow e\nu$ decay angular distribution should reveal the maximal parity violation asymmetry expected for pure V-A coupling, i.e. the positron from a W^+ decay should be preferentially emitted in the direction of the incident antiprotons and the electron of a W^- decay in the direction of the protons. For a Drell-Yan process (and without sea-sea contribution), we obtain the following decay angular distribution in the centre-of-mass-system of the W :

$$\frac{dN}{d\,\cos\theta_e^*} = (1 + \cos\theta_e^*)^2 \; ,$$

if θ_e^* is defined as the angle between the electron (positron) and the proton (antiproton) direction.

Fig. 8 shows the experimental decay angular distribution of the W, after background subtraction and correction for acceptance and resolution effects and for the bias in choosing p_L^ν (which is necessary for the Lorentz transformation, see section 4.2). Only events with a well

determined lepton charge (to better than 2 standard deviations from infinite momentum, $\Delta p/p < 2\sigma$) are considered. It is in good agreement with the expected $(1 + \cos\theta_e^*)^2$ curve for pure V-A coupling, and one can even see the effect of the small sea-sea contribution of about 2 to 4 % (depending on the choice of structure functions and indicated by the shaded band in fig. 8) in the data.

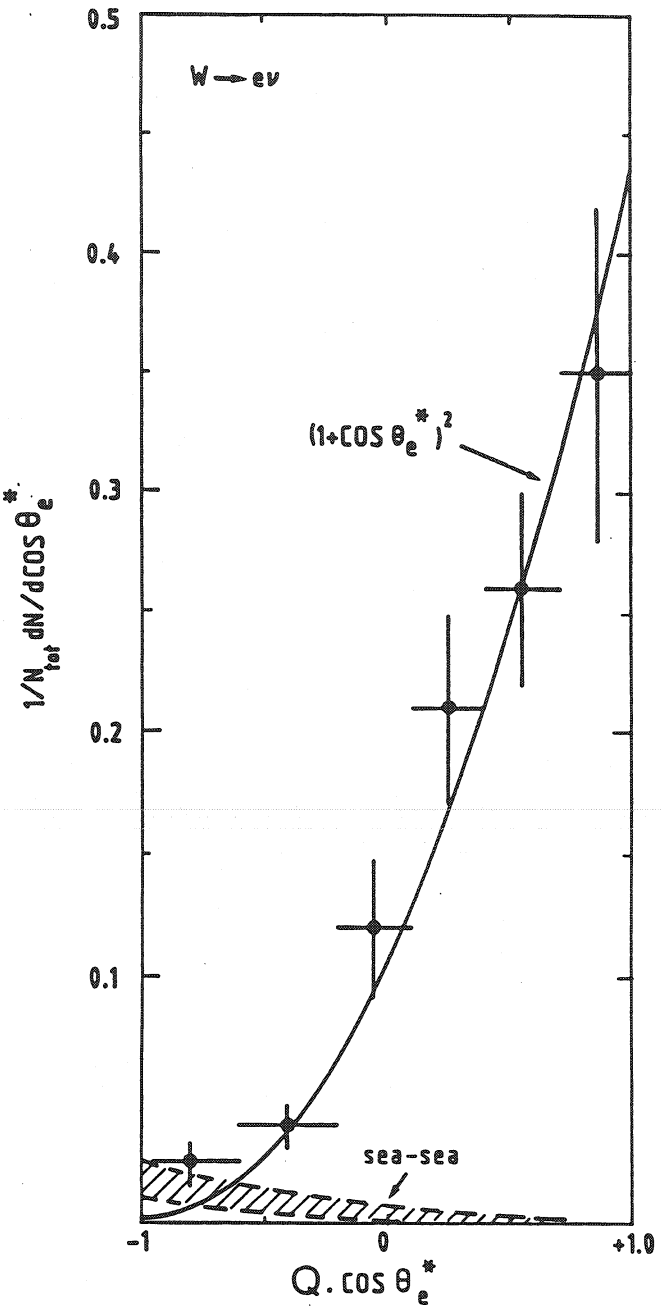

Fig. 8 : Experimental decay angular distribution of the W, after background subtraction and correction for acceptance and resolution effects and for the bias in choosing p_L^ν. Indicated is also the sea-sea contribution as a shaded band.

It can be shown [18], that the mean value of this distribution is directly correlated to the spin J of the W :

$$\langle Q \cdot \cos\theta_e^* \rangle = \frac{\langle \lambda \rangle \langle \mu \rangle}{J\,(J+1)} \quad \text{for } J > 0$$

$$= 0 \qquad \text{for } J = 0$$

where μ and λ are respectively the global helicity of the production system (ud) and the decay system ($e\nu$).

The measured value of $\langle Q \cdot \cos\theta_e^* \rangle$ is 0.43 ± 0.07, while 0.5 is expected for a spin 1 of the W and states of maximal helicity ($\langle \lambda \rangle = \langle \mu \rangle = \pm 1$) without sea-sea contribution, and 0.46 ± 0.02 by taking into account a sea-sea contribution as indicated in fig. 8. This is in excellent agreement with the data. Notice that the observed decay asymmetry is too pronounced for $J_W \geq 2$, indicating therefore unambiguously the W spin as 1.

4 - TESTS OF QCD

Until now, the Standard Model (electroweak + QCD) seems to describe well the nature. Still open questions are the top quark and the Higgs sector.

Especially, the electroweak part of the Standard Model is well established now, theoretically and exprimentally.

The QCD part is more delicate to study because of the quark confinement. However, the W statistics is now high enough to study QCD more in detail at $Q^2 \simeq M_W^2$.

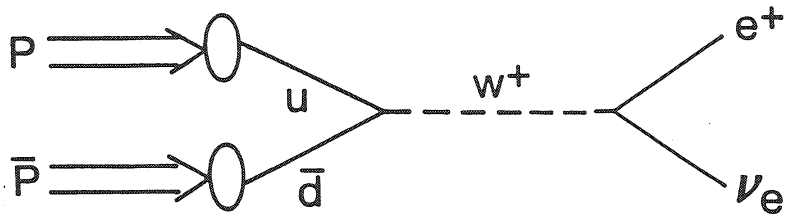

Fig. 9 : Drell-Yan production process of a W.

Fig. 9 shows the Drell-Yan production process of a W (at lowest order QCD). To calculate the production cross section :

$$\frac{d\sigma}{dx_W} = \frac{\pi\, g^2}{4\, M_W^2} \cdot \frac{x_1 \cdot x_2}{\sqrt{x_W^2 + 4\tau}} \cdot \frac{1}{3} \cdot \left\{ \left[u_1(x_1)\, \bar{d}_2(x_2) + \bar{d}_1(x_1)\, u_2(x_2) \right] \cos^2\theta_c \right.$$

$$\left. + \left[u_1(x_1)\, \bar{s}_2(x_2) + \bar{s}_1(x_1)\, u_2(x_2) \right] \sin^2\theta_c \right\}$$

where $\tau = \frac{M_W^2}{s} = x_1 \cdot x_2$, g is the coupling constant and θ_c the Cabbibo angle, it is necessary to know the parton momentum distributions u(x), d(x) etc.. They can be extracted from deep inelastic scattering experiments. The function $F_2(x) = x \cdot \sum_{\text{flavours}} e_i^2\, q^i(x)$ can be measured in deep inelastic e/μ-nucleon scattering. In the QCD improved parton model q^i depends also on Q^2: $q^i(x, Q^2)$. With our W events we can in particular test QCD at $Q^2 \simeq M_W^2$ and for $x \simeq \frac{M_W}{\sqrt{s}} \simeq 0.15$ at $\sqrt{s}$ = 630 GeV.

4.1 Production cross sections

Fig. 10 shows the experimental production cross sections a) for W and b) for Z compared to the QCD prediction of Altarelli et al. [7].

The errors on the data come mainly from the uncertainty of the luminosity (about 15 %) and are therefore correlated.

The indicated uncertainty of about 25 % on the theoretical cross

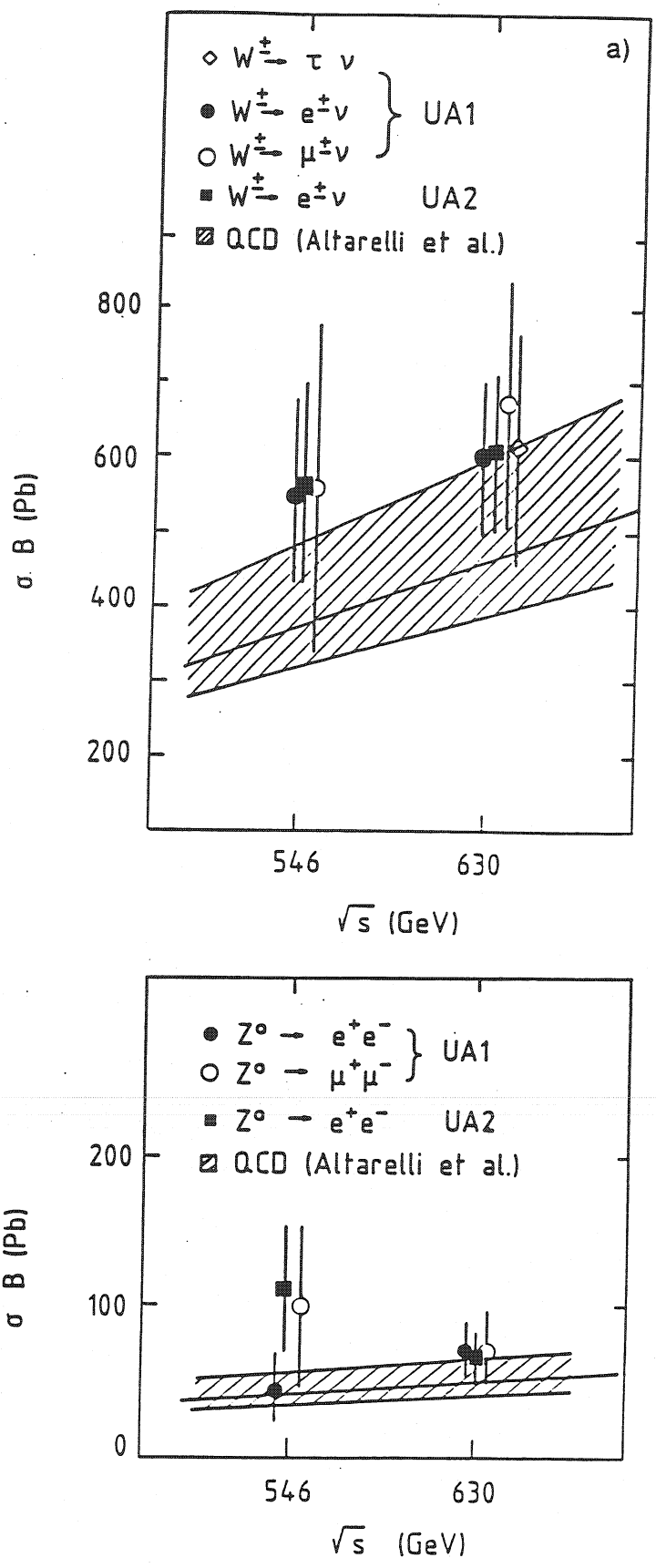

Fig.10 : Experimental production cross-sections
a) for W and b) for Z compared to the QCD prediction of Altarelli et al. [7].

section is due to the choice of the structure functions (GHR, DO1, DO2) and of Λ (Λ = 0.2 or 0.4 GeV). Furthermore, the change of the Q^2 scale in α_s from $\alpha_s(M^2_{W,Z})$ to $\alpha_s(p^2_{TW,Z})$ increases the contribution of higher orders to the cross sections. For this reason, the error on the calculated cross section is asymmetric.

As visible in fig. 10 there is an overall agreement between the data and the theory. But the experimental cross sections seem nonetheless to be systematically higher (by about 25 %) than the theoretical predictions both for the different W-decay channels of UA1, and for UA2, and at both values of $\sqrt{s}$.

One can find two possible reasons leading to an increase of the theoretical value of $\sigma.B$:

1) The branching ratios $B(W \to \ell\nu)$ and $B(Z^\circ \to \ell^+\ell^-)$ increase with the top quark mass, as shown in fig. 11 [8]. In the original prediction of Altarelli et al. [7], this mass was taken as 40 GeV/c^2, which yields :

$$B(W \to \ell\nu) = 0.089 \quad \text{and} \quad B(Z^\circ \to \ell^+\ell^-) = 0.032.$$

But it is now rather likely that the top quark is more massive. The experimental limit at this moment coming from UA1 data is $m_{top} \gtrsim 45$ GeV/c^2 [19]. Notice that for $m_{top} > m_W$, the relative increase of $B(W \to e\nu)$ is as large as $\simeq$ 20 %.

2) From the recent results on the deep inelastic structure functions $F_2^p(x,Q^2)$ at high $\langle Q^2 \rangle$ ($\simeq$ 80 GeV^2) from the experiment NA4 of the BCDMS Collaboration [20], there is a clear indication that the quark momentum distributions in current use (GHR [21], DO1 [22], EHQL1 [23]) are underestimated by about 10 % in the x-region responsible for the W and Z production ($\langle x_{W,Z} \rangle \simeq 0.15$ at $\sqrt{s}$ = 630 GeV) [5].

To illustrate this point, figs. 12 a), b) and c) show the ratios of $F_2(x)^{H_2}_{BCDMS} / F_2(x)^p$ for the 3 different parametrizations GHR, DO1 and EHQL1 as a function of x, and for each x, the ratio is calculated at the appropriate $\langle Q^2 \rangle$. In the region of $x \simeq x_{W,Z} \simeq 0.15$, the most favorable parametrization (GHR) seems nonetheless to underestimate the experimental quark momentum distribution by about 10 %. This implies

that a W,Z production cross section calculated with more appropriate parton distributions, which would be in good agreement with these at present most accurate BCDMS data, would lead to an increase of the predicted cross sections by $\simeq$ 20 % as :

$$\sigma_{W,Z} \sim \int u(x_1)\, \bar{d}(x_2)\, \delta(x_1 x_2 - M_W^2/s)\, dx_1 dx_2 .$$

Of course, a combination of both effects, namely a larger top mass (> 40 GeV/c^2), with consequently larger branching ratios, and more appropriate structure functions, softer than the present ones, i.e. larger at $x \simeq 0.15$ and smaller at $x \simeq 0.5$ as suggested by the above analysis, both these effects might conspire to increase $\sigma^{th}_{W,Z}$, as shown in fig. 13, where the predictions of Altarelli et al. (at 630 GeV) increased by 20 % are combined with the m_{top} dependence of the branching ratios. The theoretical uncertainty was not changed in percentage, but if one trusts the latest results of BCDMS and one recomputes the cross sections using a parametrization of their data, the uncertainty could be considerably reduced according to their systematical errors (60 MeV on Λ_{QCD}).

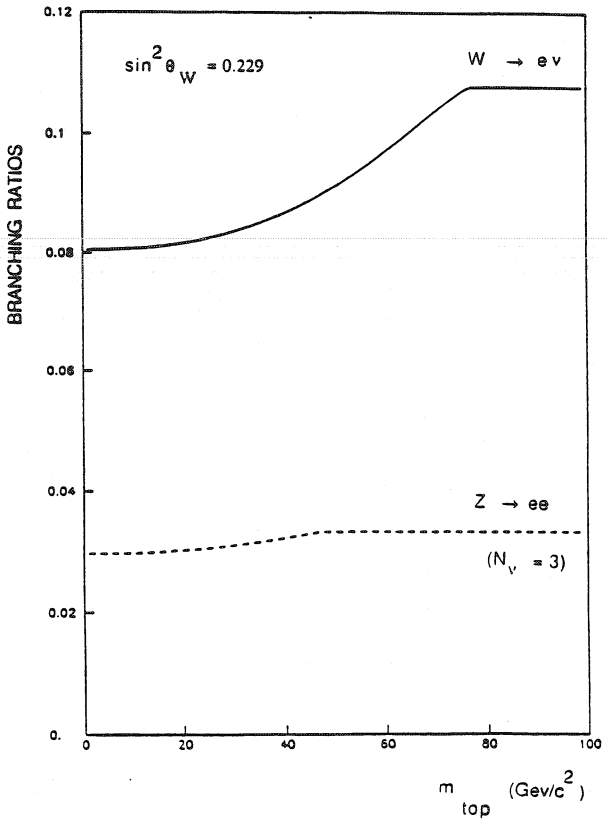

Fig.11 : Branching ratios B(W → $\ell\nu$) and B(Z° → $\ell^+\ell^-$) as a function of the top quark mass [8].

Fig.12 : Ratios $F_2(x)^{H_2}_{BCDMS} / F_2(x)^{p}$ of data to theoretical parametrizations

a) GHR, b) D01

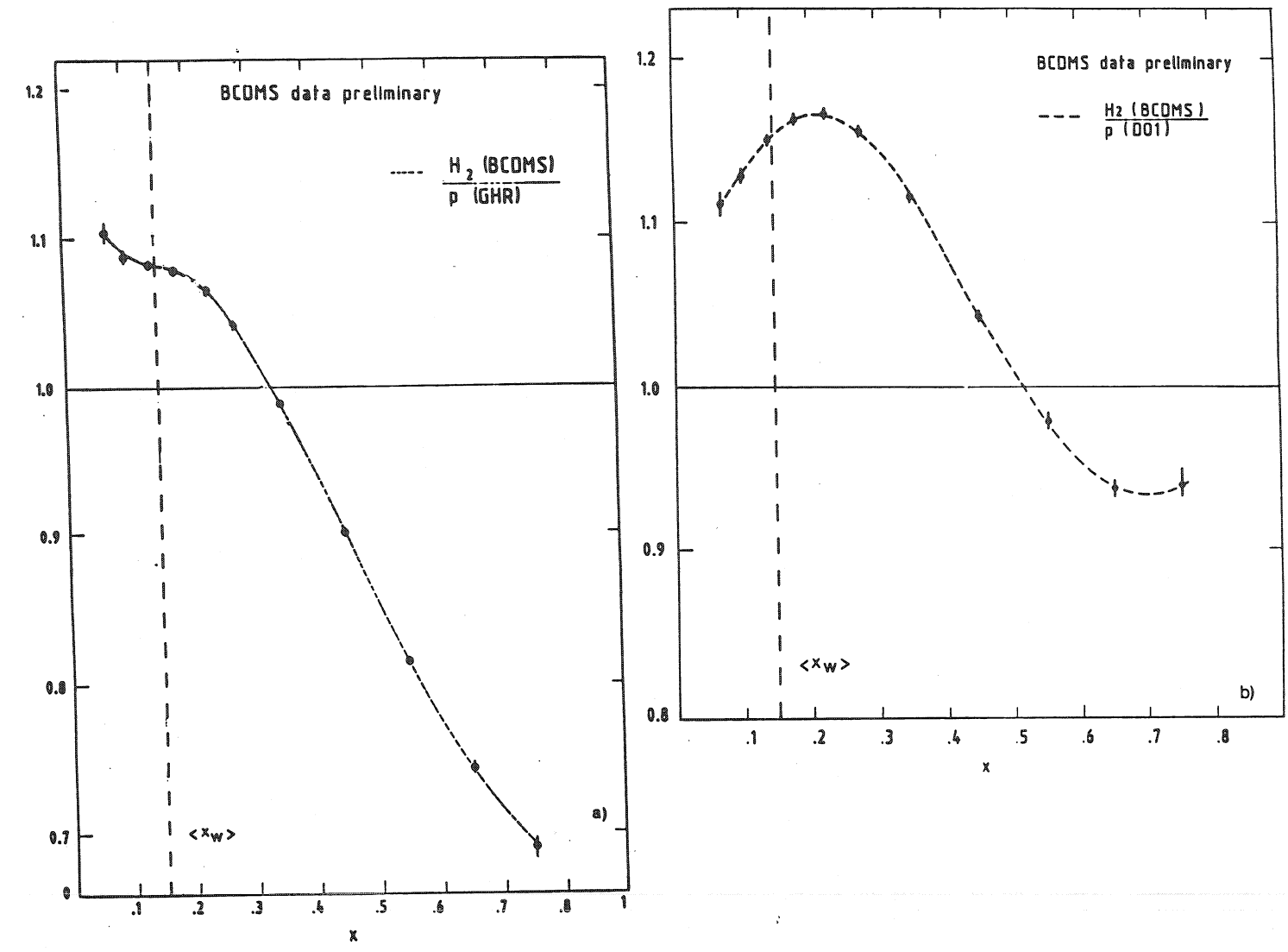

and c) EHQL1.

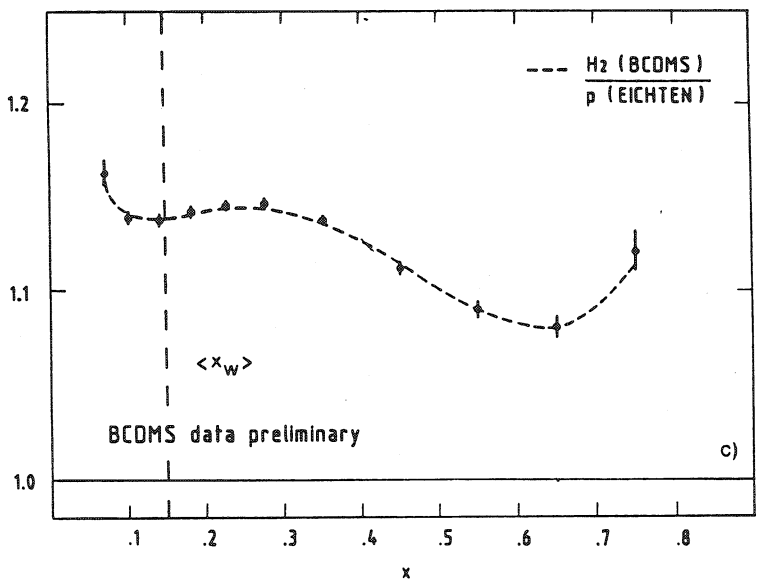

However, the overall agreement between the data and QCD represents an important confirmation of the colour quantum number, since colour suppresses the W,Z cross sections by a factor 6 (factor 3 in σ and another factor $\simeq$ 2 in the leptonic branching ratios B) [5].

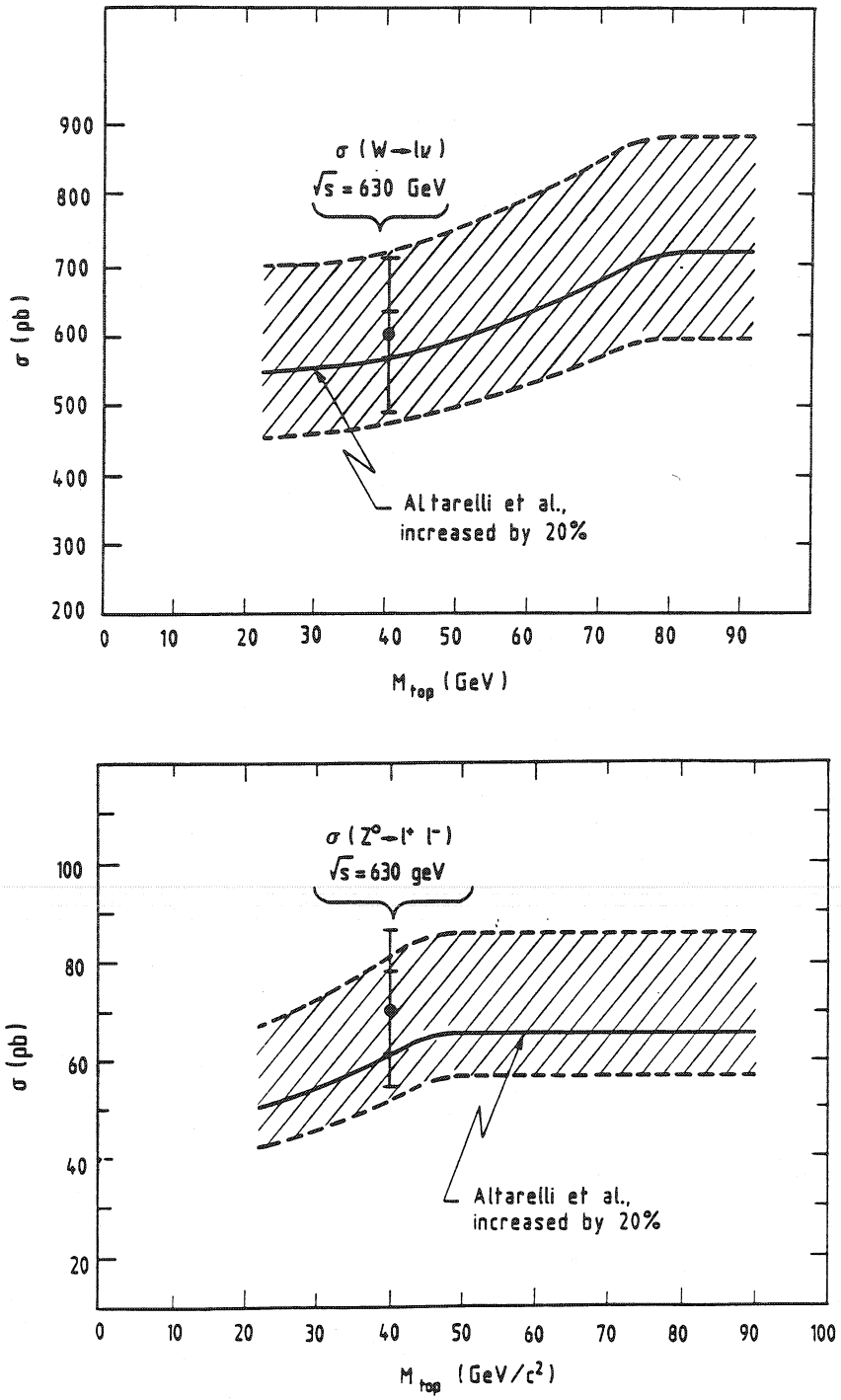

Fig.13 : Theoretical prediction of Altarelli et al. for W and Z production cross-sections, rescaled by 20 % as suggested by BCDMS data, as a function of m_{top}, with its uncertainty (hatched band), compared to the average value measured by UA1 and UA2 at $\sqrt{s}$ = 630 GeV.

4.2 The longitudinal motion of the W.

The longitudinal momentum of the W arises from the difference between the fractional momenta (x_q , $x_{\bar{q}}$) of the two annihilating quarks. It can be determined by the sum of the longitudinal momenta p_L^ν and p_L^e of the two decay leptons. Thus the Feynman x of the W is :

$$x_W \equiv x_{\bar{q}} - x_q = \frac{p_L^\nu + p_L^e}{\sqrt{s} / 2} \quad .$$

Even, if the longitudinal momentum p_L^ν of the neutrino cannot be measured directly by the experiment, it can be calculated by imposing the W mass on the electron neutrino system : $M_W^2 = (E_e + E_\nu)^2 - (\vec{p}_e + \vec{p}_\nu)^2$.

The two solutions for the neutrino longitudinal momentum p_L^ν leave us with a two-fold ambiguity for the W longitudinal momentum in about half of the events (in the other cases one of the two solutions is either unphysical ($|x_W| > 1$), or both solutions give the same value of x_W). By considering the constraint of energy conservation in the overall interaction, we choose the p_L^ν solution with the minimal total energy unbalance in the event ($\min (\sum_i \vec{E}_i)$) [5].

Since a W^+ is produced by the annihilation of a u quark and a $\bar{d}$ antiquark (and $\bar{u}d \to W^-$) , the x_W distribution is expected not to be symmetric with respect to zero, so far as u and d momentum distributions differ at $Q^2 \simeq M_W^2$.

If we consider the $Q \cdot x_W$ distribution (with Q the W charge sign, and the positive x axis along the incident $\bar{p}$ direction), then the $Q \cdot x_W < 0$ hemisphere corresponds to W production, where the fractional momentum of the u quark is larger than that of the d quark, and conversely for the $Q \cdot x_W > 0$ hemisphere. The experimental $Q \cdot x_W$ distribution is shown in fig. 14 a), after background subtraction and correction for acceptance and resolution effects and for the bias in choosing p_L^ν [5]. Only events with a well determined lepton charge (to better than 2 standard deviations from infinite momentum, $\Delta p/p < 2\,\sigma$) are considered. The

asymmetry of the corrected experimental distribution is in good agreement with the expectations that the u quarks contributing to the W production are in general "harder" than the d quarks (χ^2 = 8 for 7 degrees of freedom). For comparison we show the expected distribution using EHQL1 structure functions. Our data are not sensitive, however, to the various choices of structure functions (EHLQ, DO, GHR).

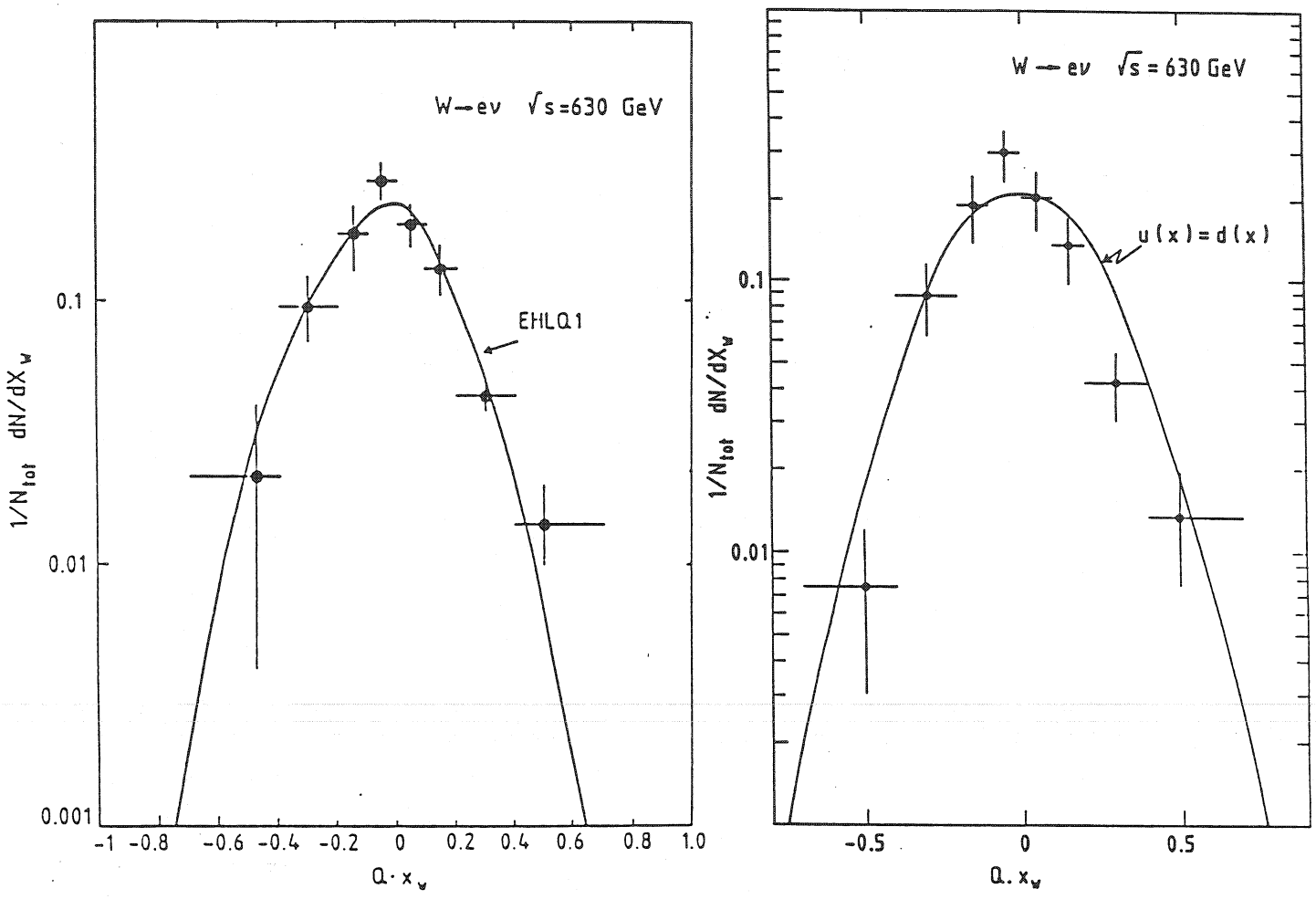

Fig.14 : Experimental $Q \cdot x_W$ distribution after background subtraction and correction for acceptance and resolution effects and for the bias in choosing p_L^ν, for :

a) EHQL1 structure functions at $Q^2 = M_W^2$, and
b) with the assumption u(x) = d(x).

In fig. 15 we show the correction factor applied. It is obtained by a Monte Carlo technique and is given by the ratio of generated to reconstructed and selected $W \to e\nu$ events. Its form is quite asymmetric : There are more events lost with $Q \cdot x_w < 0$ than events with $Q \cdot x_w > 0$. This is due to the combination of three effects :

i) the V-A coupling of the W producing a very asymmetric decay distribution,

ii) the fact that the u quark is usually harder than the d quark resulting in an average boost of the W in the direction of incident u($\bar{u}$)and

iii) the requirement of a well measured charge Q_e, which, due to our dipole $\vec{B}$ field, eliminates preferentially events with $\theta_e^{lab} \simeq 90°$.

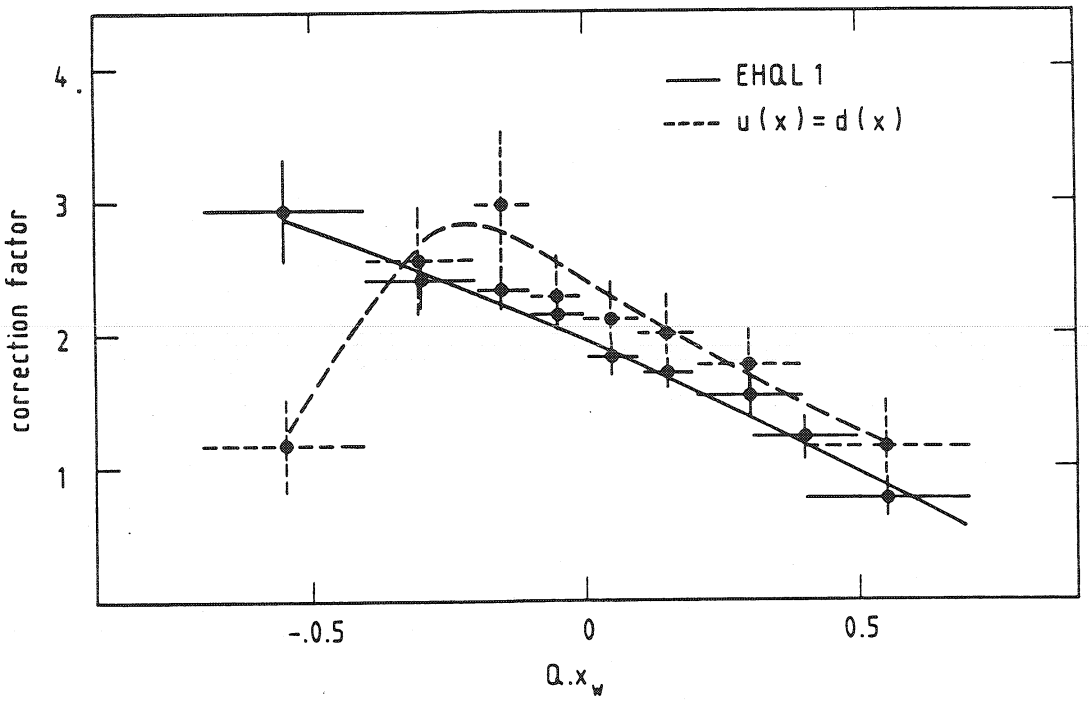

Fig.15 : Correction factor obtained by a Monte Carlo technique.

If we assume equal fractional momentum distributions for the u and d quarks, the correction factor is less asymmetric (dashed line in fig. 15) and the resulting corrected experimental distribution is compared in fig. 14 b) to the theoretical expectation assuming $u(x) = d(x)$, ($\chi^2 = 23$ for 7 degrees of freedom). This is therefore direct evidence that $u(x)$ is indeed harder than $d(x)$ at $Q^2 \simeq M_W^2$.

From the relation $x_q \cdot x_{\bar{q}} = M_W^2/s$ and knowing the charge of the W, one can determine separately the x_u and x_d distributions contributing to W production. They are shown in fig. 16 a) and b), after background subtraction and correction for acceptance and resolution effects and for the bias in choosing p_L^ν. The mean values are : $\langle x_u \rangle = 0.17 \pm 0.01$ and $\langle x_d \rangle = 0.13 \pm 0.01$, and the shapes of the x_u and x_d distributions, as sampled by W production, are in good agreement with the expectations.

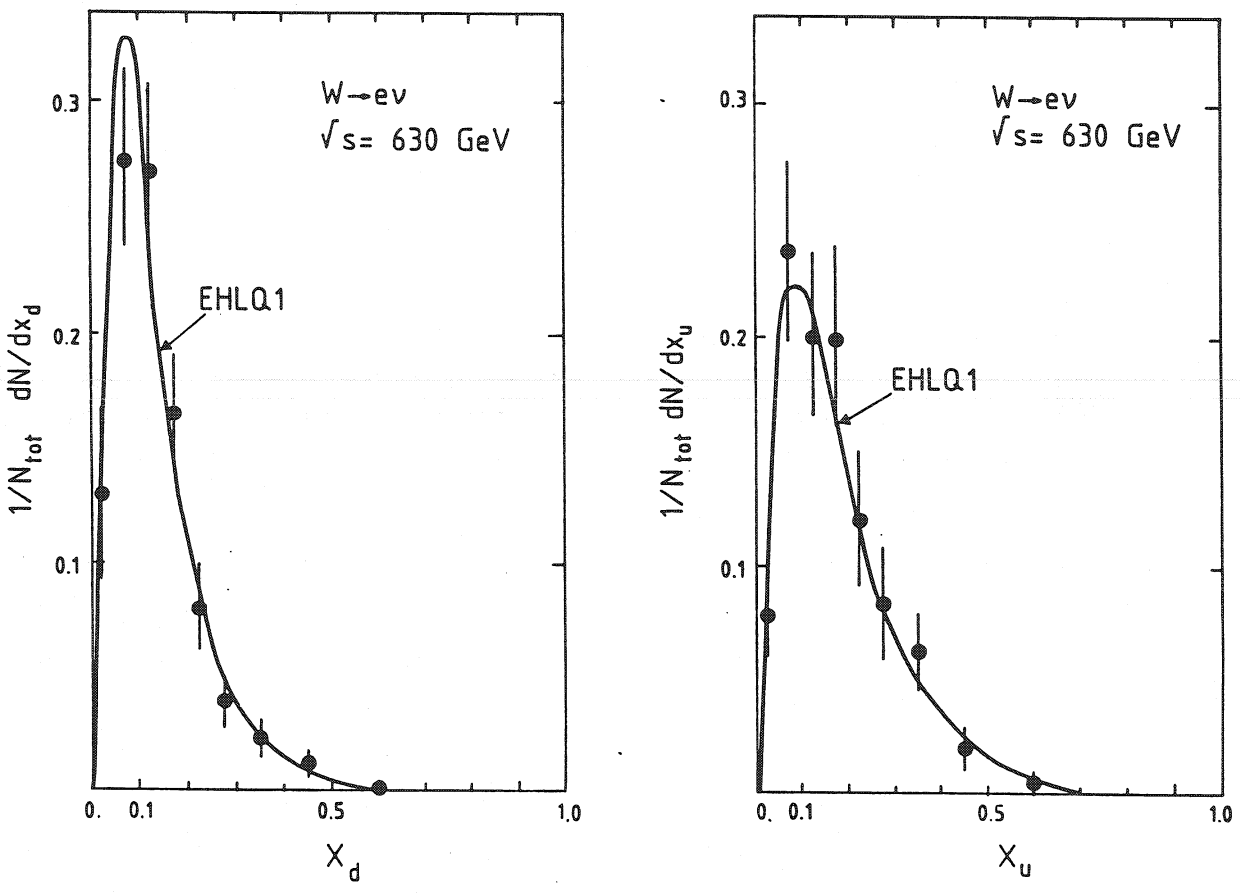

Fig.16 : a) x_u and b) x_d distributions contributing to W production, after background subtraction and correction for acceptance and resolution effects and for the bias in choosing p_L^ν.

4.3 The transverse momentum of the W

In a first approximation, the vector bosons W and Z are produced by the Drell-Yan mechanism of quark-antiquark annihilation. In the QCD improved picture of the production mechanism quarks and antiquarks can radiate gluons thus generating a recoil transverse momentum for the W and Z. So, higher-order corrections must be taken into account for the correct description of the observed $p_T^{W,Z}$ distributions. If the radiated gluons, responsible for the p_T of the W or Z, have a sufficiently high transverse energy, they produce observable jets in our apparatus. These jets are reconstructed by the standard UA1 jet algorithm [24].

In fig. 17 the observed transverse momentum distribution of the W is shown. The distribution has a peak at $\sim$ 4 GeV/c, and then has a long tail up to $p_T^W \simeq M_W$, resulting from the gluon emission. It is well described by the QCD calculations of Altarelli et al. [7] using the structure functions of DO1 [22] with Λ = 0.2 GeV , modified for experimental acceptance and resolution effects. In a simple Drell-Yan parton model this distribution would be very narrow and concentrated near zero, the entire p_T^W being then due only to the intrinsic quark transverse momenta. Indeed, as indicated in fig. 17 (hatched area), a large fraction of W events have a recognizable jet (of $E_T \geq 5$ GeV) produced in association with the W. This is the case for almost all events with $p_T^W > 10$ GeV/c.

The shape of the theoretical transverse momentum distribution of the W depends on the parametrization of structure functions, the choice of Λ_{QCD} and the Q^2 scale in α_s [7], especially in the region $p_T^W \lesssim 25$ GeV/c. In fig. 18 two theoretical p_T^W distributions, modified for experimental acceptance and resolution effects [5], with different sets of structure functions and Λ_{QCD} are compared to the data at $\sqrt{s}$ = 630 GeV. We notice that the data are contaminated by a $\sim$ 10 % background, which is concentrated at small p_T^W and has been subtracted in fig. 18 [5]. One can see that in this intermediate p_T^W range the QCD calculation describes well the data, and there is a hint that the distribution with Λ_{QCD} = 0.2 GeV is favoured (χ^2 = 17 for 10 degrees of freedom) compared to the curve with Λ_{QCD} = 0.4 GeV (χ^2 = 22 for 10 degrees of freedom).

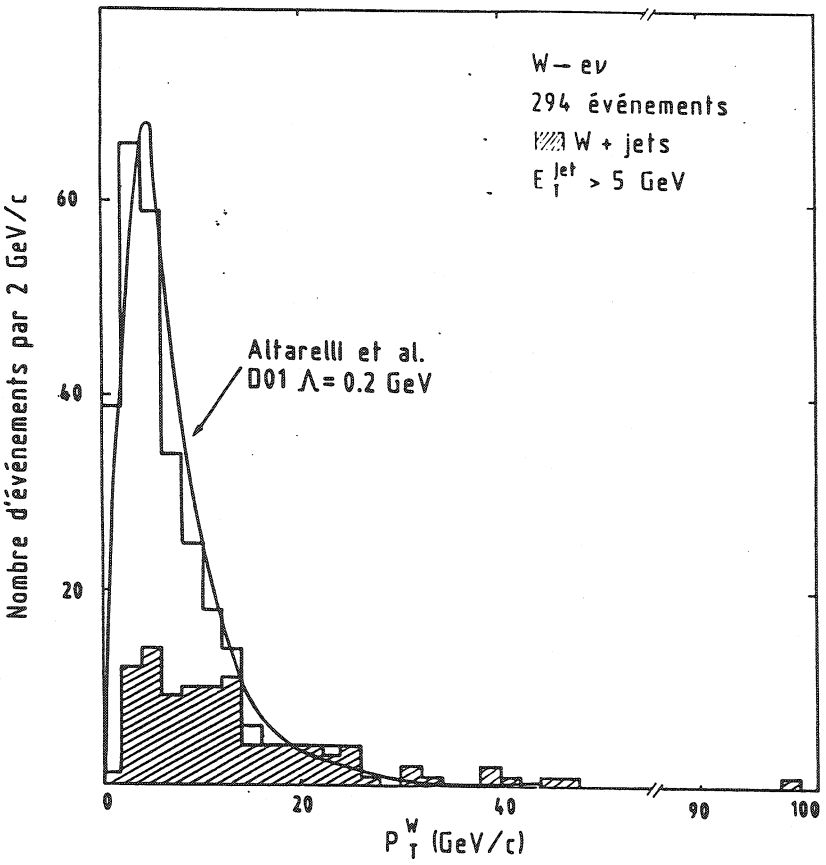

Fig.17 : Experimental transverse momentum distribution of the W compared to the QCD prediction of Altarelli et al., which is modified for acceptance and resolution effects. Also indicated (hatched area) the fraction of W events with at least one jet ($E_T^{jet} \geq 5$ GeV).

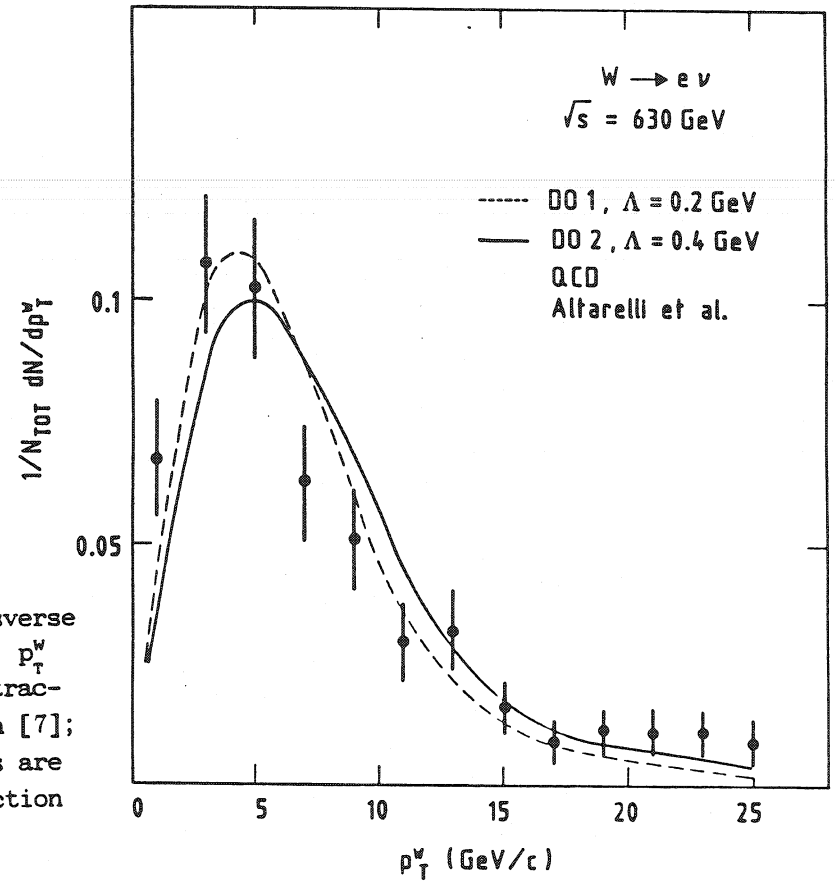

Fig.18 : Normalised experimental W transverse momentum distribution for $p_T^W \leq 26$ GeV/c with background subtracted, compared to QCD prediction [7]; the theoretical distributions are modified to account for selection and apparatus effects.

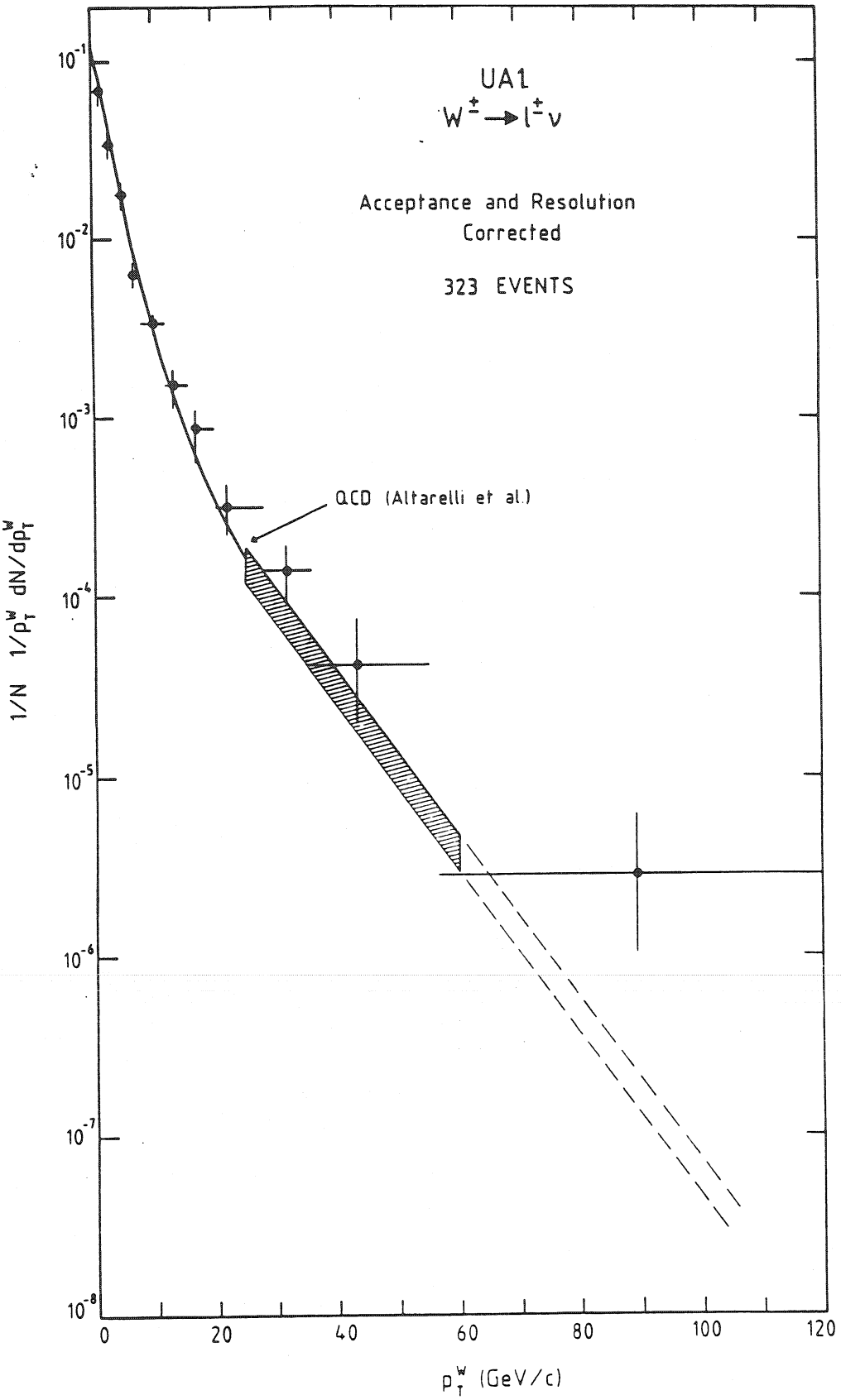

Fig.19 : Experimental $1/N \; 1/p_T^W \; dN/dp_T^W$ distribution, corrected for acceptance and detector resolution, compared to QCD predictions [7] with extrapolations based on ISAJET (dashed lines) for $p_T^W > 60$ GeV/c.

For a comparison of the data in the region of large transverse momentum with perturbative QCD calculations, it is more practical to choose a logarithmic scale. Fig. 19 shows the experimental spectrum $1/N_{tot}\ 1/p_T^W\ dN/dp_T^W$, after background subtraction and correction for acceptance and resolution effects, compared to the QCD calculation of Altarelli et al. [7]. The hatched region beginning with $p_T^W \geq 25$ GeV/c is the perturbative calculation of Altarelli et al. with the uncertainties largely connected to the choice of the Q^2 scale to be used in α_s. This calculation was extended from 65 GeV/c up to 120 GeV/c by a Monte Carlo [25]. Within the errors, the experimental W transverse momentum distribution is in good agreement with the QCD predictions up to the highest p_T^W values of order M_W. A graphical representation of the two W events with highest transverse momentum ($p_T^W \simeq 100$ GeV/c in the electron channel and $p_T^W \simeq 80$ GeV/c in the muon channel) is shown in fig. 20. They have both two jets recoiling against the W, with jet-jet effective masses of ~ 95 GeV and ~ 80 GeV and W-jet-jet masses of ~ 280 GeV and ~ 300 GeV respectively. These events are discussed in more detail in [26], but at this level of statistics, only speculative interpretations are possible [27].

The transverse momentum distribution of the Z events is shown in fig. 21. It has a similar shape and again events accompanied by at least one jet have in average a higher p_T^Z (shaded events in fig. 21).

QCD predicts that the average transverse momentum of lepton pairs produced in Drell-Yan processes increases linearly with the energy $\sqrt{s}$ for constant $\sqrt{\tau}$ ($\tau = M^2/s$) [28] :

$$\langle p_T^2 \rangle = \alpha_s(\ln Q^2) \cdot s \cdot f(\tau, \ln Q^2) + c,$$

where f is a structure function.

This implies : $\langle p_T \rangle \sim \sqrt{s}$ (to logarithmic terms) at fixed τ, so far as the Q^2 dependence ofα_s and f is slow (logarithmic).

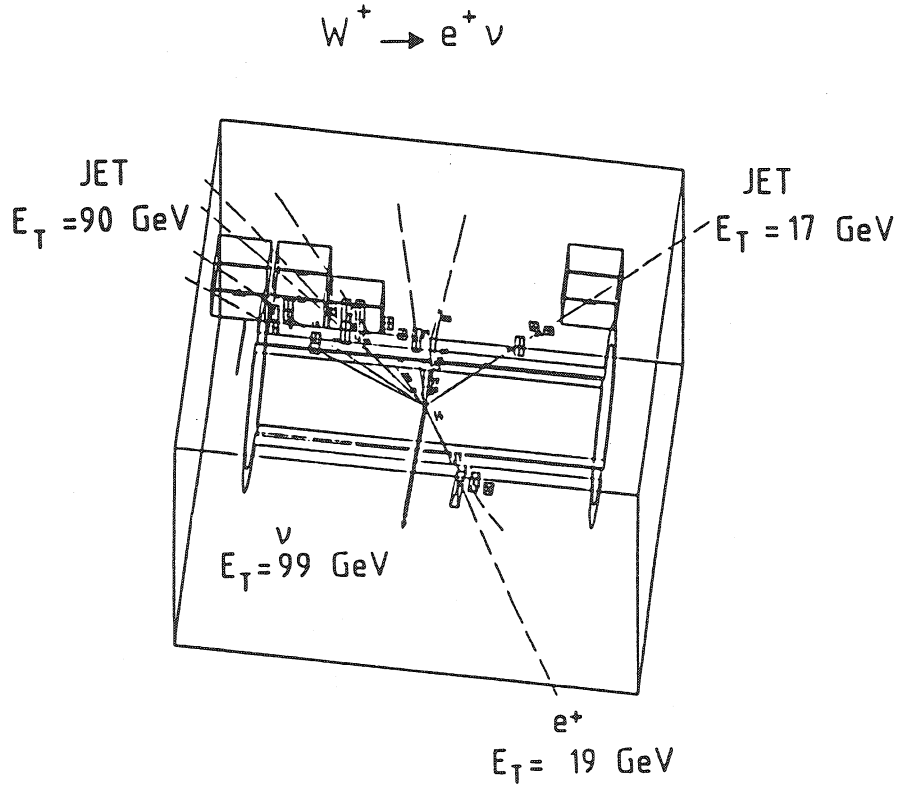

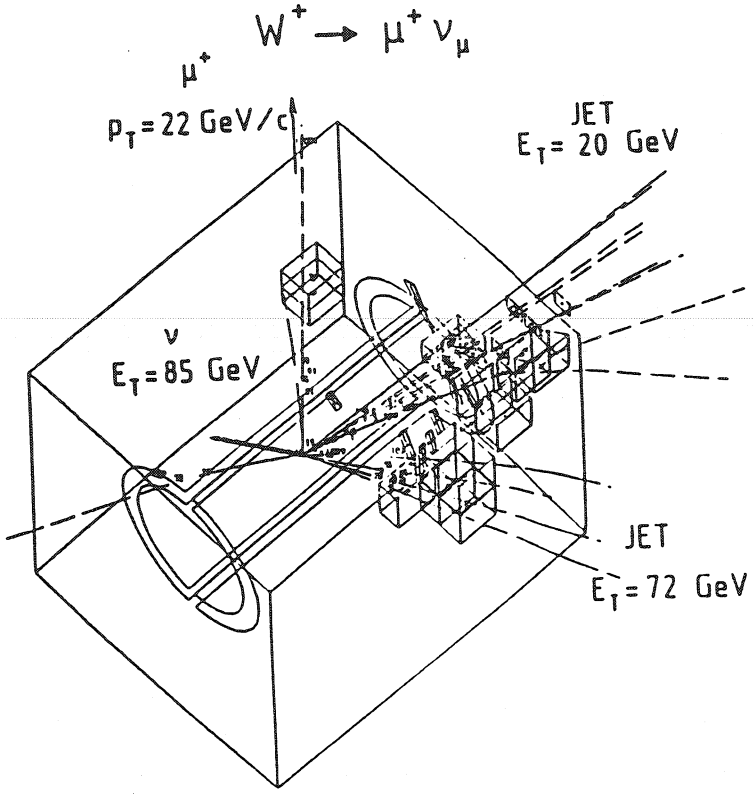

Fig.20 : Graphic display of the calorimeter cells (E_T > 1 GeV) and charged tracks (p_T > 1 GeV/c) observed in the UA1 detector for the highest transverse momentum W events a) in the electron channel and b) in the muon channel.

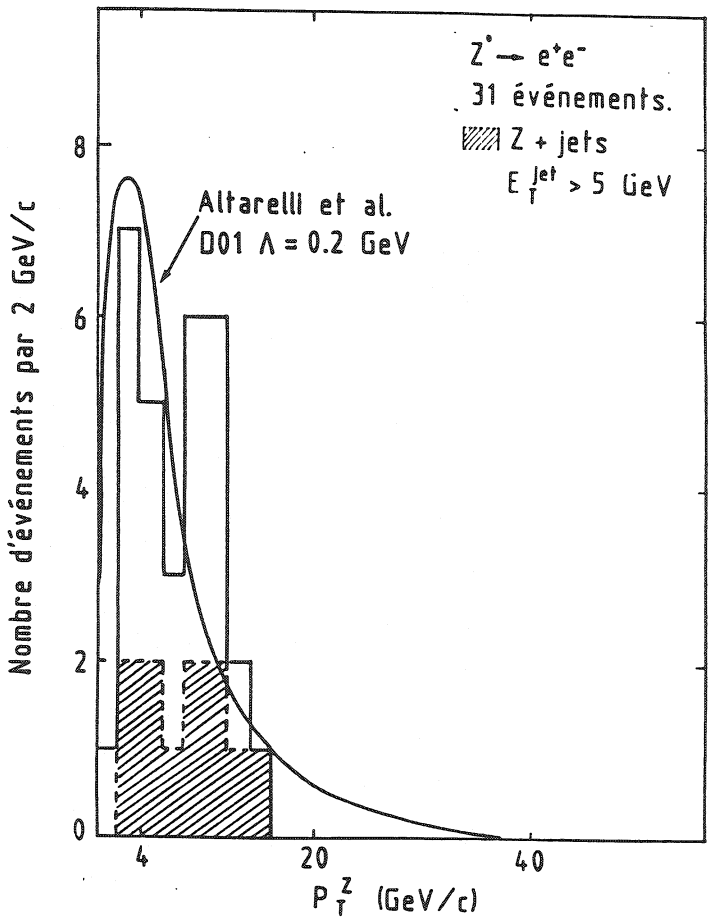

Fig.21 : Experimental transverse momentum distribution of the Z° events compared to the QCD prediction of Altarelli et al., which is modified for acceptance and resolution effects. Also indicated (hatched area) the fraction of Z° events with at least one jet ($E_T^{jet} \geq 5$ GeV).

Fig. 22 shows the $\sqrt{s}$-dependence of the average transverse momentum values of lepton pairs in Drell-Yan processes : in the region of $\sqrt{s} \lesssim 62$ GeV the data are taken from [29] and [30] at $\sqrt{\tau} = 0.22$; $\langle p_T^W \rangle$ and $\langle p_T^Z \rangle$ are also shown at $\sqrt{s} = 540$ GeV and $\sqrt{s} = 630$ GeV, which corresponds to $\sqrt{\tau} \simeq 0.15$, close enough to the kinematical region of $\sqrt{\tau} = 0.22$ for a comparison [28]. The errors on $\langle p_T^{W,Z} \rangle$ from UA1 contain also the systematic uncertainty on the absolute energy scale (± 8 % for the W). Over the whole range of $\sqrt{s}$ up to 630 GeV, the data are in good agreement with a linear extrapolation of the QCD prediction [28].

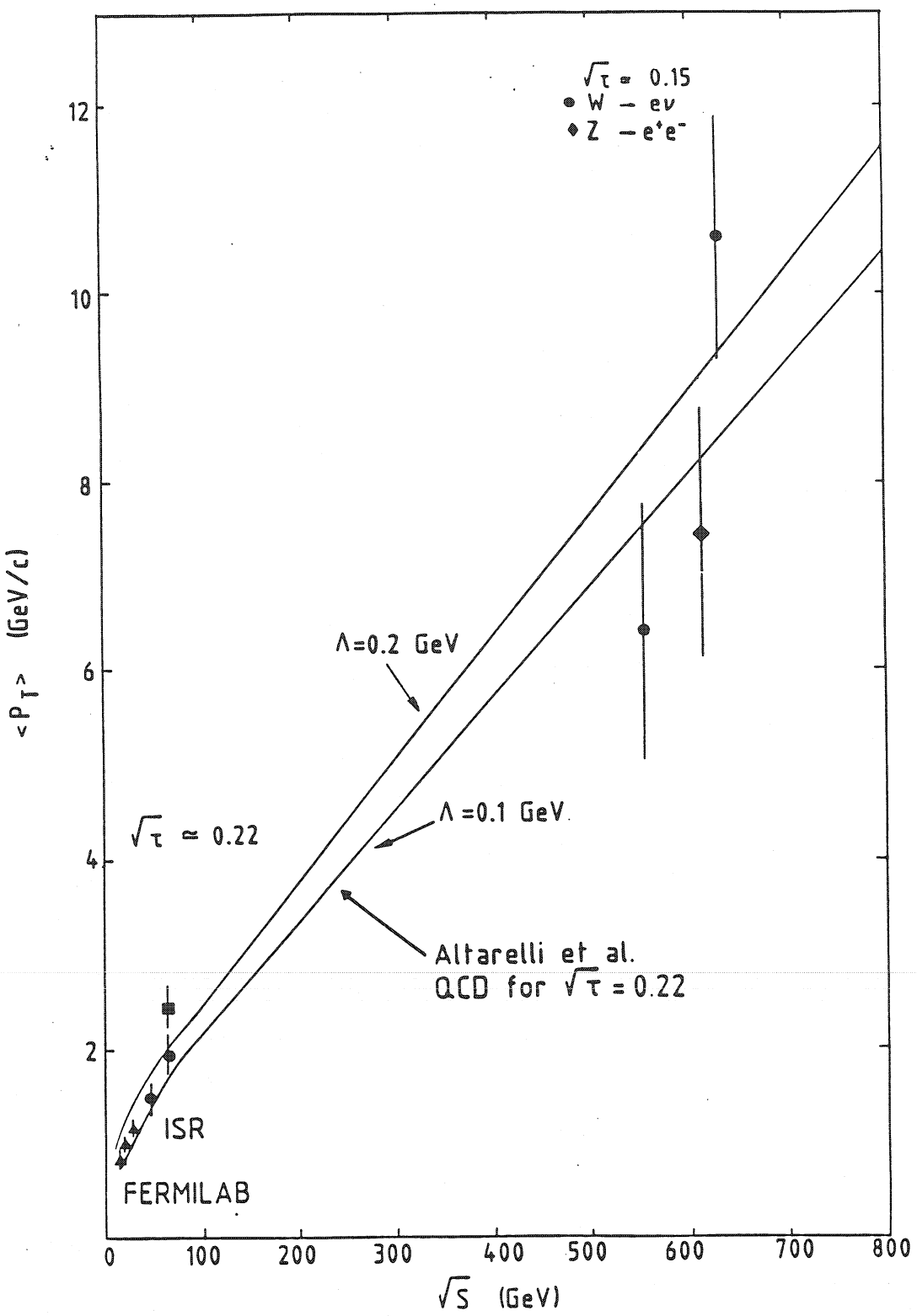

Fig.22 : Average momentum values of lepton pairs in Drell-Yan processes as a function of $\sqrt{s}$ [28], data coming from [29] and [30] and from W and Z° events.

4.4 Jets associated to W/Z production

After the observation of jets in the final hadronic state X of W/Z events : $p\bar{p} \rightarrow W/Z + X$, it is interesting to study in more detail the structure of this inclusive state X.

The jet multiplicity distributions, for jets of $E_T > 5$ GeV produced in association with W's and Z's, are shown in fig. 23. They are compared to the QCD expectations of Stirling et al. [31], where the probability for n-jets is approximately the n^{th} power of the one-jet probability. The jet activity in the W events is the same as in the Z events, within the statistical errors.

To illustrate the correlation between the W transverse momentum and the jet multiplicity, the average number of jets with $E_T > 5$ GeV (or 10 GeV) is represented as a function of p_T^W in fig. 24. The average jet multiplicity increases with the W transverse momentum up to ~ 2, with however the softer jet close to the cut-off value of 5 GeV.

4.5 Test of the gluon spin

A method to test the gluon spin has been suggested in ref. [32] making use of the axial-vector coupling of the intermediate vector bosons $W^{\pm}$. Since the axial part of the current is not generally conserved, the polarization state of a W produced in association with a single gluon is sensitive to the gluon spin. The polarization state of the W can be measured through the W decay angular distributions [33,34]:

$$\frac{1}{2}\,\frac{d\,N_{e\,+\,\nu}}{d\cos\theta} = \frac{3}{8}\left(1 + \frac{A_0}{2}\right)\left[1 + \frac{2 - 3\,A_0}{2 + A_0}\cos^2\theta\right]$$

$$\frac{1}{2}\,\frac{d\,N_{e\,+\,\nu}}{d\varphi} = \frac{1}{2\pi}\left[1 + \frac{A_2}{4}\cos 2\varphi\right].$$

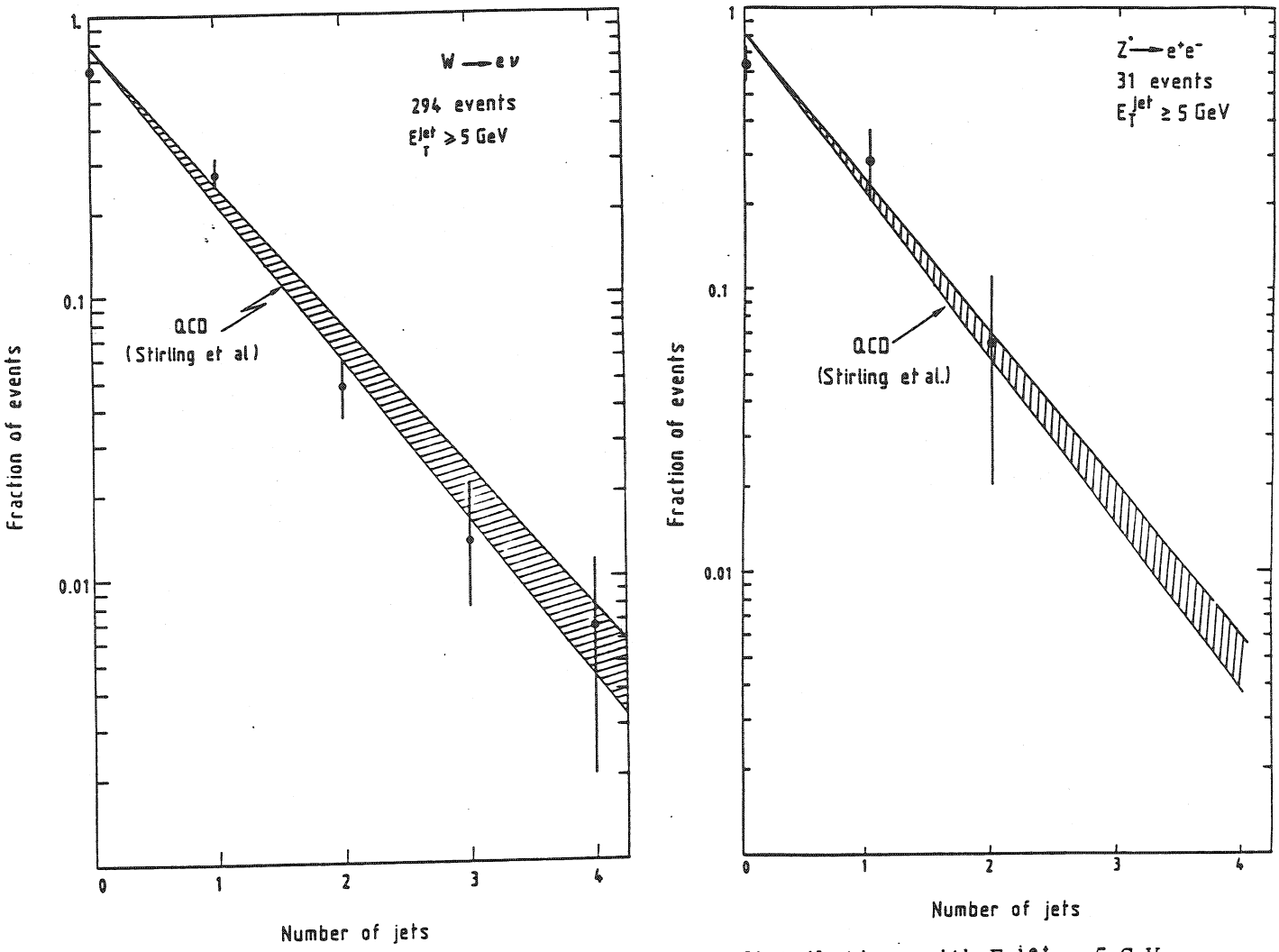

Fig.23 : Experimental jet multiplicity distributions with $E_T^{jet} > 5$ GeV compared to QCD predictions [31] for a) $W \to e\nu$ events and b) $Z^\circ \to e^+e^-$ events.

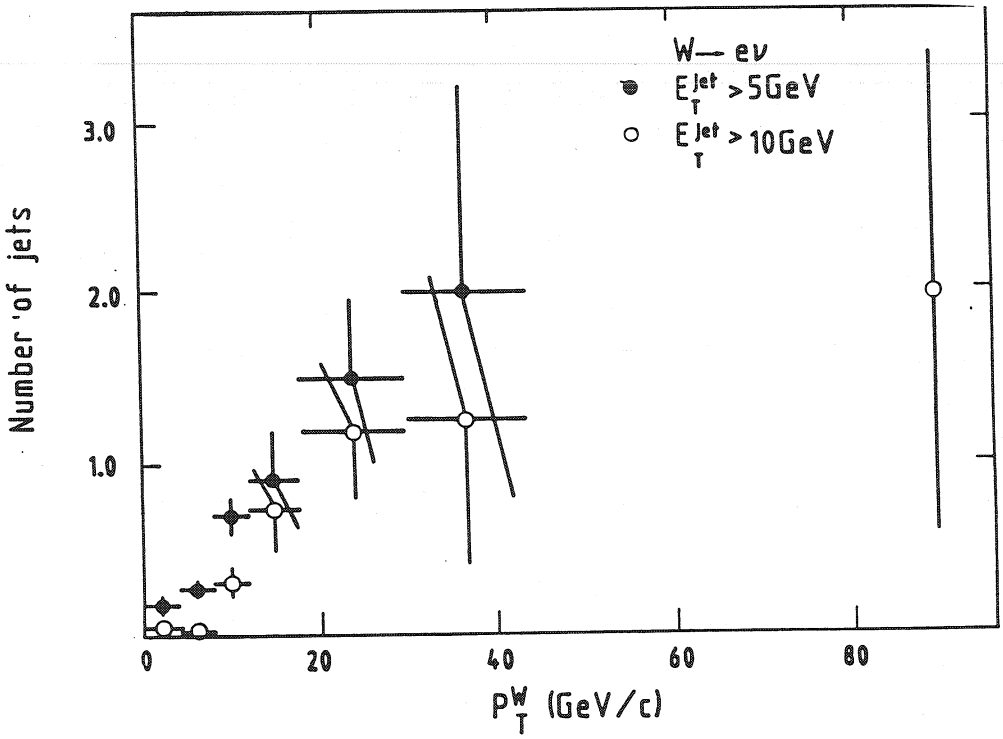

Fig.24 : Average number of jets with $E_T > 5$ GeV (or 10 GeV) as a function of p_T^W .

The angles φ and θ are the azimuthal and the polar angle of the electron momentum in the $W^{\pm}$ rest frame. A_0 and A_2 are combinations of the helicity amplitudes of the W [32] .

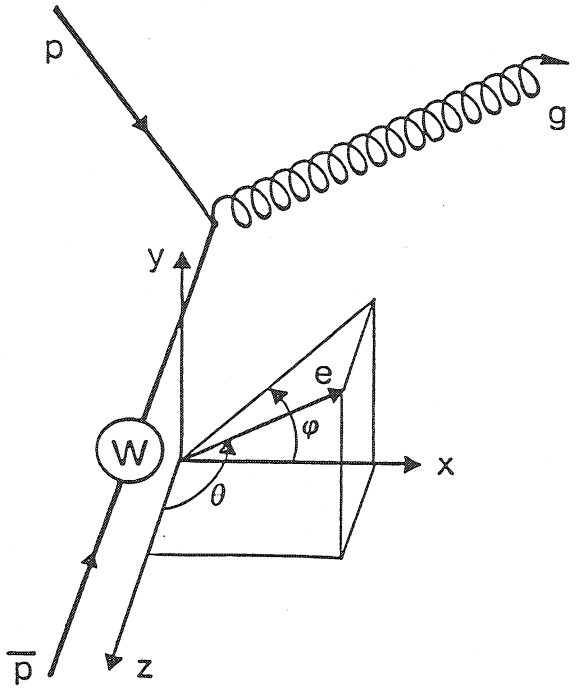

Fig.25 : The Gottfried-Jackson frame
The Gottfried-Jackson is defined in the following way : beginning with the quadrivectors of the leptons, the proton and the antiproton one performs a Lorentz-transformation into the centre-of-mass system of the lepton pair ($\hat{=}$ $W^{\pm}$). Then one takes the CMS-momentum of the antiproton and define its direction as the z-axis. The vector product of the proton-momentum with the antiproton-momentum gives the y-axis and the cross product of this vector with the z-vector gives us the x-axis.

The theoretical prediction, in one specific W rest frame - the Gottfried-Jackson frame (see fig. 25) -, is $A_0 - A_2 = 2$ for a scalar gluon (changing the quark helicity) and $A_0 - A_2 = 0$ for a vector gluon (preserving the quark helicity). One can see in ref. [32], that the cos θ distribution is particularly sensitive to the gluon spin. In our p_T^W region (p_T^W between $\sim$ 10 and $\sim$ 30 GeV/c), we should expect :

$$\frac{dN}{d|\cos\theta|} \sim 1 + \cos^2\theta \qquad \text{for a vector gluon}$$

and :

$$\frac{dN}{d|\cos\theta|} \sim 1 - \cos^2\theta \qquad \text{for a scalar gluon.}$$

This means that in the case of a vector gluon the decay leptons are preferentially emitted in the direction of the beams, as predicted in a simple Drell-Yan process, whereas the polarization state of the W will be strongly disturbed by a scalar gluon and the decay leptons should be emitted preferentially in the central region.

For the determination of A_0 and A_2 we have to select W events with a (single) hard gluon emission. To save statistics, a cut $p_T^W \geq 7$ GeV/c is chosen, which leaves us with a sample of 121 W's out of 294 W's. Nearly all these events do indeed have observable jets reconstructed by the UA1 jet algorithm [24]. Since the resolution of the p_T^W measurement is about 3 GeV/c, we are cutting at λ 2 σ from $p_T^W = 0$.

Since we are interested in W events with the emission of a single gluon, we also eliminate events with more than one recognizable jet (jet threshold is $E_T^{jet} \geq 5$ GeV). That leaves in our final sample for this analysis 111 $W \to e\nu$ events. Although this cut does not eliminate events with multigluon emission, where gluons have not enough energy to create recognizable jets, it is not critical for the analysis because on the one hand, multigluon emission is strongly suppressed in theories with scalar gluons [35], and on the other hand, in the case of vector gluons, multigluon emission does not change the result, since it does not affect the original decay lepton angular distribution.

A study of the dependence of the background on p_T^W shows, that the region with $p_T^W \geq 6$ GeV/c is practically background free [5], so we do not need to subtract any background from this data sample.

Finally, the experimental decay angular distributions are corrected for acceptance losses and the effects of detector resolution and of the p_L^ν ambiguity described above by a correction factor obtained from a detailed Monte Carlo simulation of the apparatus [25]. For the experimental cos θ distribution, we must apply two different correction factors : one corresponding to the vector gluon hypothesis and the other

corresponding to the scalar gluon hypothesis used in the Monte Carlo.

The experimental lepton angular distributions with the fitted functions are shown in fig. 26 for φ and in fig. 27 a) and b) for cos θ, the data being corrected separately for the two different gluon spin hypotheses.

The results for the fitted parameters A_2 and A_0 are the following :

1) The φ distribution yields $A_2 = 0.08 \pm 0.60$

2) From the cos θ distribution we obtain :

a) for the vector gluon hypothesis $A_0 = -0.19 \pm 0.32$.

The expected distribution for a vector gluon ($A_0 \approx 0$) is also shown in fig. 27 a) -dashed line, and a comparison to the data gives : $\chi^2 = 3$ for 4 degrees of freedom

b) for the scalar gluon hypothesis $A_0 = 0.70 \pm 0.35$.

Fig. 27 b) -dashed line, shows also the expected distribution for a scalar gluon ($A_0 \approx 2$) compared to the data with : $\chi^2 = 15$ for 4 degrees of freedom.

This then leads to the final results :

$$A_0 - A_2 = -0.27 \pm 0.68$$

to be compared to $A_0 - A_2 = 0$ for a vector gluon

and $$A_0 - A_2 = 0.62 \pm 0.69$$

to be compared to $A_0 - A_2 = 2$ for a scalar gluon.

By the method described here, the vector character of the gluon is confirmed. A scalar gluon can be excluded at a $\sim 2\ \sigma$ level from the $(A_0 - A_2)$ measurement, independent of p_T^W . But since in the limited p_T^W region of our data, A_0 is not expected to vary too much [32], it is possible to exclude the scalar gluon hypotheses even at a $\sim 4\ \sigma$ level from the A_0 measurement alone.

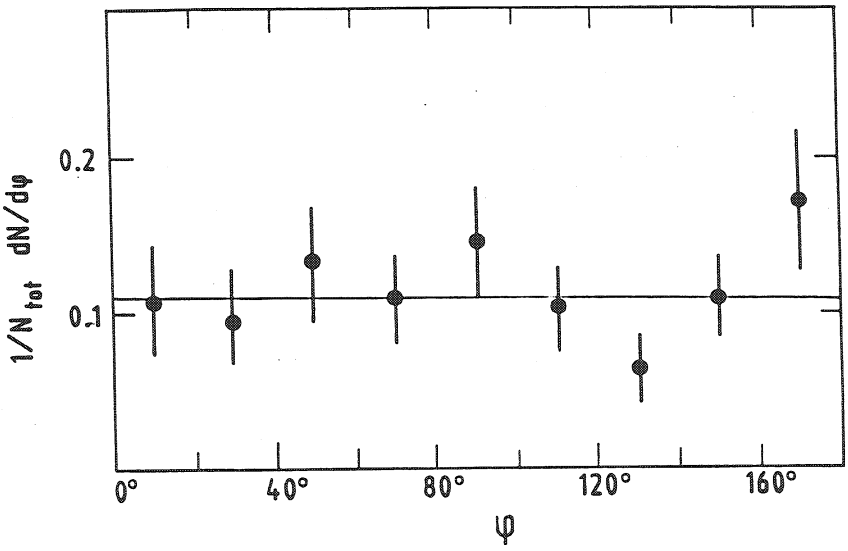

Fig.26 : Azimuthal W-decay angular distribution in the Gottfried-Jackson frame for $p_T^W \geq 7$ GeV/c, data corrected for acceptance and resolution effects.

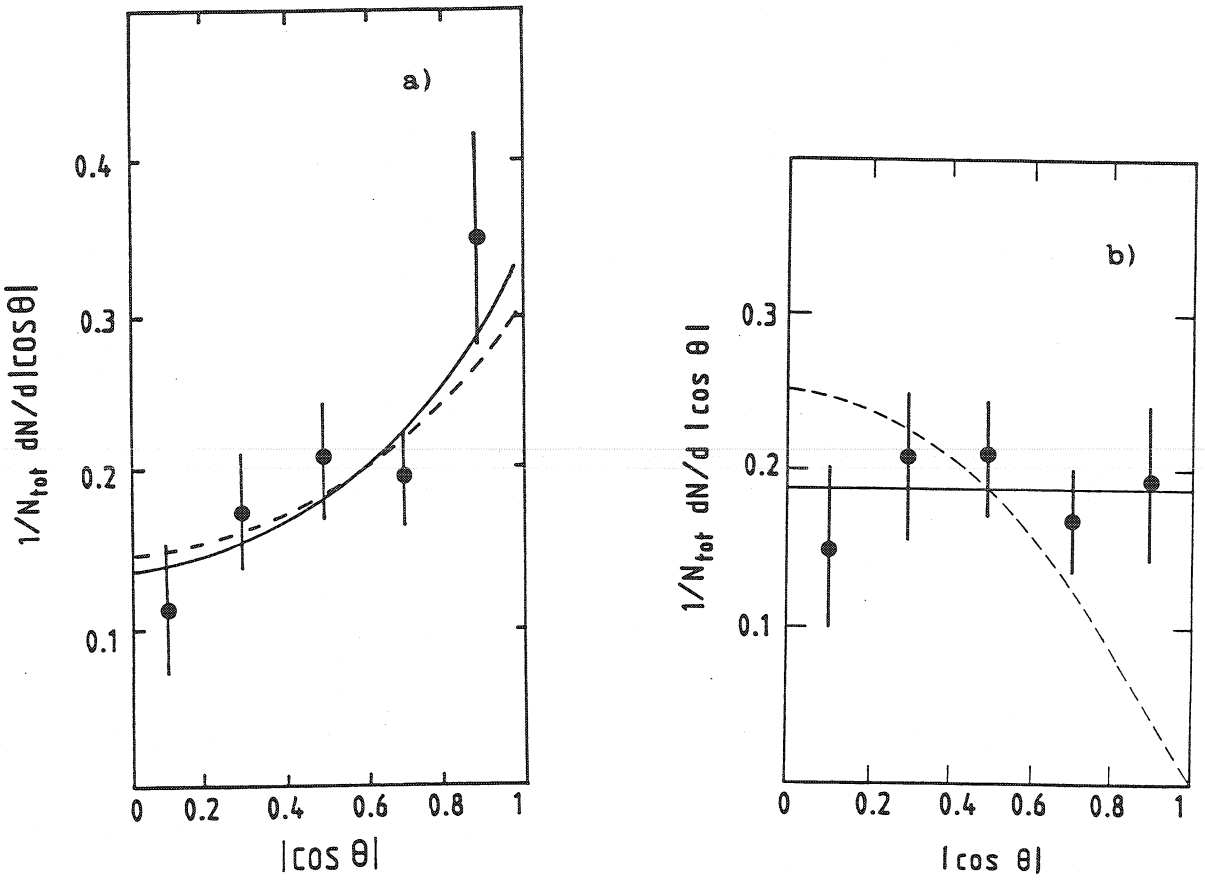

Fig.27 : Polar W-decay angular distribution in the Gottfried-Jackson frame for $p_T^W \geq 7$ GeV/c, data corrected for acceptance and resolution effects

a) for vector gluon hypothesis,

b) for scalar gluon hypothesis.

The solid line is the best fit to the data, the dashed line is the theoretical expectation for the chosen gluon spin assignment.

Therefore, in addition to the gluon spin determination based on three-jet event correlations in e^+e^- annihilations at PETRA [36] and with two-jet event angular distributions in UA1 [37], this is another independent method showing the internal consistency of QCD through the spin 1 assignment for the gluon [38].

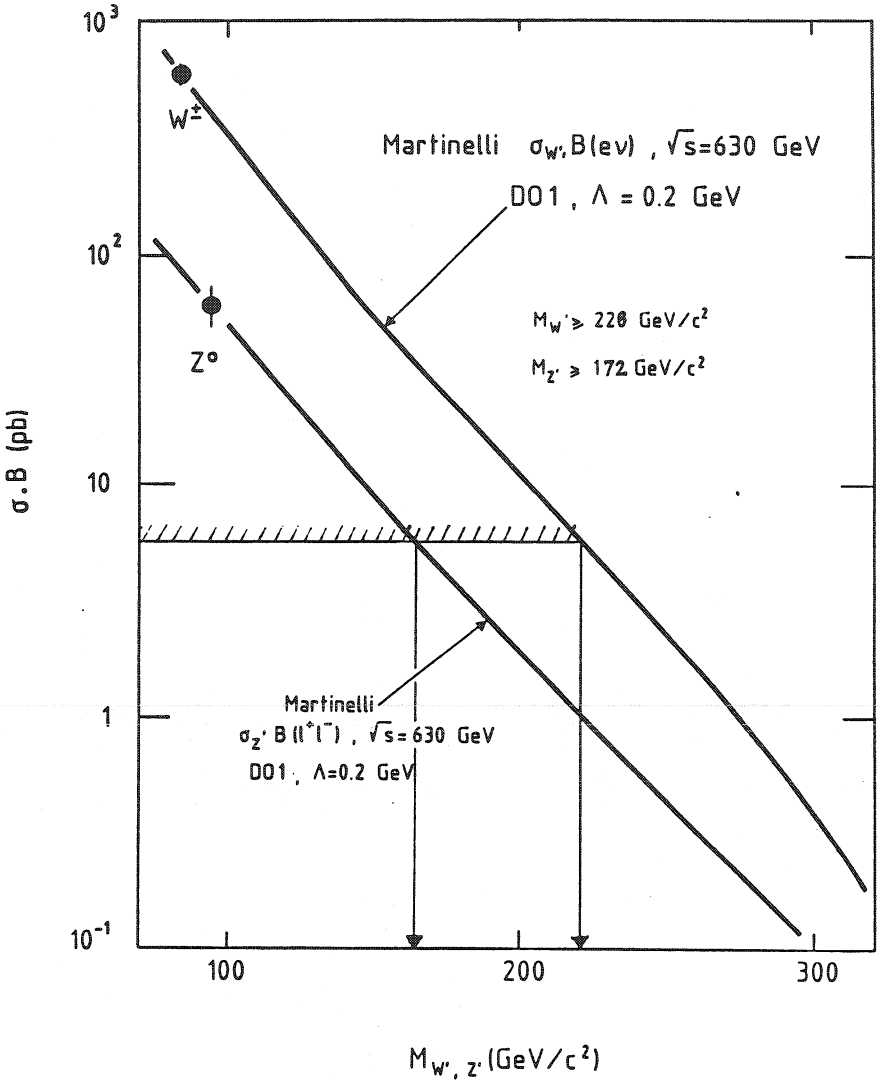

Fig.28 : Production cross-sections for heavy vector bosons W' and Z' as a function of their mass.

5 - EXOTICS

Since with present statistics, UA1 has not observed any new particles predicted in theories other than the Standard Model, we review in this paragraph just the mass limits on "not-Standard Model-particles".

From figs. 6 and 5 we see, that no electron-neutrino nor electron-positron pair has been observed with a transverse mass $m_T^{e\nu}$ or an effective mass m_{ee} larger than predicted in the Standard Model.

The experimental sensitivity limits of UA1 for more massive intermediate vector bosons, expected for example in some left-right symmetric models, are 4.9 pb for objects of type $Z' \to e^+e^-$ and 4.9 pb for $W' \to e\nu$ (at 90 % C.L.). By assuming that these hypothetic W' and Z' are coupled to quarks and leptons like the standard W and Z, and that they have the same branching ratios in $e\nu$ and e^+e^-, the calculation by Martinelli et al. [39] (see fig. 28) gives the following mass limits :

$$M_{W'} > 226 \text{ GeV/c}^2$$

$$M_{Z'} > 172 \text{ GeV/c}^2 \qquad \text{at 90 \% C.L.}$$

The superymmetric particles $\tilde{e}$ and $\tilde{\nu}$ could be detected by observing the W decay : $W \to \tilde{e} + \tilde{\nu}$, with the selectron decaying into an electron and a photino (assuming the photino to be the lightest supersymmetric particle). Such a W decay would have softer electron and neutrino energy spectra, and in particular the electron angular distribution would be very different. Since our observed E_T^e, E_T^ν and decay angular distributions after background subtraction are well described by (V-A) expectations for $W \to e\nu$ decay [5], one gets the following mass limits (assuming $m_{\tilde{e}} = m_{\tilde{\nu}}$) [40] :

$$m_{\tilde{e},\tilde{\nu}} > 30 \text{ GeV/c}^2 \qquad \text{at 90 \% C.L.}$$

6 - CONCLUSIONS

The study of the production and decay properties of about 400 W's and 40 Z's provides new results on lepton universality and on the upper limit on the number of neutrino species as well as more incisive tests of the electroweak part of the Standard Model and especially of QCD at a very high $Q^2 \simeq M_W^2$:

- The comparison of the production cross-sections in the decay $W \to e\nu$, $W \to \mu\nu$, $W \to \tau\nu$, as well as $Z^\circ \to e^+e^-$ and $Z \to \mu^+\mu^-$, verifies for the first time lepton universality in weak currents at $Q^2 = M_{W,Z}^2$, and this at a better than 25 % level for cross sections (or better than 11 % level in terms of weak couplings).

- The upper limit on the number of (light) neutrinos varies from 7 to 4 (at 90 % C.L.) with a top quark mass increasing from 40 to 80 GeV/c^2. By combining the results of UA1 and UA2, the limit is more constraining : 6 to 3 (at 95 % C.L.).

- The masses and decay widths of the weak bosons are in good agreement for the different decay channels and also with the results of UA2. They are a little bit higher than the theoretical predictions of SU(2) x U(1) at lowest order, indicating the presence of the expected radiative corrections. Unfortunately, we are not yet sensitive enough to measure precisely these radiative corrections. The measured Standard Model parameter $\sin^2\theta_W$ is in good agreement with the most accurate results from deep inelastic neutrino scattering and ρ is compatible with 1, at a $\lesssim 4$ % level.

- The decay angular distribution of the charged boson W is consistent with pure V-A coupling. There is a hint for the small contribution to W production from sea quarks in the experimental electron decay angular distribution.

- The measured W,Z production cross sections are in good agreement with the results of UA2. Although in agreement with QCD predictions, they seem to be systematically above (by about 25 %). This could be explained either by applying a new set of structure functions (based on new results of the BCDMS Collaboration) or by taking a top quark mass higher than 40 GeV/c^2 as used in the original theoretical calculation, or by a combination of the two effects. Nonetheless, the overall agreement between the data and QCD represents an important confirmation of the colour quantum number.

- The experimental W longitudinal momentum distribution reflects the fact that the proton u quark momentum distribution is harder than for the d quark.

- The experimental W transverse distribution provides direct evidence for gluon bremsstrahlung and is in remarkable agreement with the QCD predictions up to values of $p_T^W \sim M_W$. A detailed analysis of the p_T^W spectrum in the range $\lesssim$ 25 GeV/c seems to favour the choice of Λ_{QCD} = 0.2 GeV and scale $Q^2 = M_W^2$. At $\sqrt{s}$ = 630 GeV, the average transverse momentum of the W and Z is about 9 GeV/c, entirely consistent with the almost linear increase of the average transverse momentum of lepton pairs produced in Drell-Yan process with $\sqrt{s}$, as predicted by QCD.

- The jet activity associated to W and Z production is the same. The average multiplicity of jets increases with W transverse momentum.

- The vector character of the gluon is confirmed by an analysis based on the decay angular distributions of W's produced at high transverse momentum.

- Mass limits on heavier vector bosons, the selectron and the sneutrino are obtained.

In conclusion, at our present level of statistics, all experimental distributions concerning the W and Z bosons confirm the Standard Model predictions at $Q^2 \simeq M_W^2$. We are now eager to see how the Standard Model will survive the more precise measurements we expect in the future, thanks to more statistics and better detectors. Fortunately, results will soon come, both from ACOL at CERN and at the higher energy of $\sqrt{s}$ = 2 TeV from the Tevatron at Fermilab.

References

[1] UA1 proposal, CERN/SPSC/78-06, SPSC/P92 (1978).

[2] G. Arnison et al., Nuovo Cimento Lett. 44 (1985) 1,
Phys. Lett. 166B (1986) 484.

[3] G. Arnison et al., Phys. Lett. 134B (1984) 469,
Phys. Lett. 147B (1984) 241.

[4] C. Albajar et al., Phys. Lett. 185B (1987) 233.

[5] C. Stubenrauch, Thèse d'Etat, Université Paris-Sud,
Note CEA-N-2532 (1987).

[6] R. Ansari et al., Phys. Lett. 194B (1987) 158.

[7] G. Altarelli, R.K. Ellis, M. Greco, G. Martinelli,
Nucl. Phys. 246B (1984) 12 ;
G. Altarelli, R.K. Ellis, G. Martinelli,
Z. Phys. C27 (1985) 617.

[8] P. Colas, D. Denegri, C. Stubenrauch,
CERN UA1-TN 87/18 (1987) ;
P. Colas, Thèse d'Etat, Université Paris 6 (1987) ;
F. Halzen, Phys. Lett. 182B (1986) 388.

[9] A.D. Martin, R.G. Roberts, W.J. Stirling
RAL-87-002 (1987), submitted to Phys. Lett.

[10] M. Diemoz, F.Ferroni, E. Longo and G. Martinelli,
CERN-TH 4751/87.

[11] C. Albajar et al., CERN EP 87-149,
submitted to Phys. Lett. B.

[12] E. Locci, CERN EP 87-154 (1987).

[13] S. Wimpenny, CERN EP 86-60 (1986).

[14] R. Ansari et al., Phys. Lett. 186B (1987) 440.

[15] W.J. Marciano, BNL 38-767, Proc. of the XXIII Int. Conf. on high-energy physics, 16-23 July 1986, Berkeley, CA, vol.II p. 815.

[16] Particle Data Group, Phys. Lett. 170B (1986) 1.

[17] J.V. Allaby et al., CHARM Coll., CERN-EP/86-94 (1986) ;
C. Guyot, CDHS Coll., Proc. of the 12th Int. Conf. on neutrino physics and astrophysics, Sendaï (Japan), June 3-8, 1986 p. 445 ;
F. Merritt, CCFR Coll. ibidem. p. 435 ;
R. Brock, FMMF Coll. ibidem. p. 456.

[18] M. Jacob, Nuovo Cimento 9 (1958), 826. ;
M. Jacob, CERN PRE 87-027, talk at Les Houches Winter School, 21/3 - 2/4 1987.

[19] C. Albajar et al., CERN EP 87-190,
Submitted to Zeitschrift für Physik. C.

[20] BCDMS, A. Ouraou, M. Virchaux, private communication ;
A. Milsztajn, Talk given at the International Europhysics Conference on high-energy physics, Uppsala, 25 June -1 July 1987 ;
R. Ross, Talk given at the International Symposium on lepton and photon at high energies, Hamburg, July 27-31, 1987.

[21] M. Glück, E. Hoffmann, E. Reya, Z. Phys. C13 (1882) 119.

[22] D.W. Duke, J.F. Owens, Phys. Rev. 30D (1984) 49.

[23] Eichten et al., Rev. Mod. Phys. 56 (1984) 579.

[24] G. Arnison et al., Phys. Lett. 123B (1983) 115.

[25] F.E. Paige, S. Protopopescu, ISAJET Program, BNL 29777 (1981) ;
M. Della Negra, Physica Scripta 23 (1981) 469.

[26] E. Albajar et al., Phys. Lett. 193B (1987) 389.

[27] P. Colas, D. Denegri, Phys. Lett. 195B (1987) 295.

[28] G. Altarelli, R.K. Ellis, G. Martinelli,
Phys. Lett. 151B (1985) 457.

[29] A.S. Ito et al., Phys. Rev. D23 (1981) 604.

[30] A.L.S. Angelis et al., Phys. Lett. 147B (1984) 472 ;
D. Antreasyam et al., Phys. Rev. Lett. 45 (1980) 863 ;
47 (1981) 12 ; 48 (1982) 302.

[31] S.D. Ellis, R. Kleiss, W.J. Stirling,
CERN-TH 4096/85 (1985), 4185/85 (1985).

[32] N. Arteaga-Romero, A. Nicolaidis and J. Silva,
Phys. Rev. Lett. 52 (1984) 3.

[33] M. Chaichian, M. Hayashi, and K. Yamagishi,
Phys. Rev. D25 (1982) 1.

[34] C. Stubenrauch, CERN UA1 TN 87-11.

[35] D. Bailin, A. Love, Nucl. Phys. B75 (1974) 159 ;
S. Coleman, D. Gross, Phys. Rev. Lett. 31 (1973) 851 ;
A. Zee, Phys. Rev. D7 (1973) 3630.

[36] R. Brandelik et al., Phys. Lett. 97B (1980) 453.

[37] G. Arnison et al., Phys. Lett. 136B (1984) 294.

[38] J. Ellis, and I. Karliner, Nucl. Phys. B148 (1979) 141

[39] G. Martinelli, private communication.

[40] S. Geer, Talk given at the International Europhysics Conference on High-Energy Physics, Uppsala, 25 June-1 July 1987, CERN-EP/87-163.